

# Integrated Multivariate Statistical and GIS Techniques for Assessing Groundwater Quality in Tolon and Kumbungu Districts, Northern Ghana

Delaiah Antwi Nyarko<sup>1</sup>, Larry Pax Chegbele<sup>2</sup>

<sup>1</sup>Water Management Officer, Water Resources Commission, P.O. Box CT 5630, Cantonments, Accra, Ghana

<sup>2</sup>Associate Professor, Department of Earth Science, P.O. Box LG 58, University of Ghana, Legon, Accra, Ghana

## Abstract

The study employed a comprehensive approach combining traditional graphical techniques, advanced statistical analysis, and geospatial evaluation methods to analyze groundwater data across select areas of the Tolon-Kumbungu District in Ghana's northern region. Its primary aim was to ascertain the key factors that influence the composition of subsurface water and assess its quality for domestic and agricultural purposes. The study revealed silicate dissolution and the impact of anthropogenic activities, as major contributors to regional variations in groundwater chemistry. Moreover, through the utilization of Q-mode Hierarchical Cluster Analysis (HCA) alongside Stiff diagrams, distinct water types were delineated across the groundwater flow regime: Na-Mg-HCO<sup>3</sup> in recharge areas transitioning to Na-HCO<sup>3</sup>, and eventually Na-Cl in discharge zones. Furthermore, findings from the Korjinski diagram suggested stable groundwater conditions primarily involving kaolinite, indicating limited constraints on groundwater flow. Utilizing a modified Water Quality Index approach tailored for the study region and employing an Inverse Distance Weighting (IDW) interpolation method for estimated WQIs, the study spatially classified groundwater quality as generally 'good' to 'excellent' for domestic purposes. Assessments based on Wilcox diagrams revealed that the majority of wells in the district are suitable for irrigation, yet some in discharge areas may pose concerns due to elevated salinities potentially impacting plant osmotic potentials.

**Keywords:** Hydrochemical Analysis, Multivariate Statistical Analysis, Aquifers

## 1 Introduction

Sustainable national socioeconomic development in Ghana hinges on the efficient use and management of groundwater alongside surface water resources. This encompasses their utilization in homes, irrigation, and industrial activities (Yidana et al., 2011; Yeleliere et al., 2018; Amuah et al., 2022; Hagan et al., 2022). Notably, there has been a growing reliance on groundwater for drinking purposes, particularly within developing nations (Massally et al., 2017; Seidu and Ewusi, 2018). Groundwater serves as a fundamental component of rural water supply systems, accessed at various depths to meet escalating demands. This

shift towards groundwater usage is attributed to concerns over the quality of surface water sources (Seidu and Ewusi, 2018).

While groundwater is relatively shielded from surface pollutants, making it bacteriologically suitable for many households and agricultural purposes without extensive chemical treatment, it is not immune to contamination (Sasakova et al., 2018; Masindi & Foteinis, 2021; Mahjoub et al., 2022). Human practices and advancements, including waste generated by large-scale animal farming, fertilizers, pesticides, and incidents like petroleum leaks or discharges from subsurface containment systems or wastewater reservoirs, pose threats to its integrity, safety, and sustainability (Ferrer et al., 2020; Abanyie et al., 2023). These joint impacts of environmental processes and human interventions can render groundwater resources unfit for diverse use (Akhtar et al., 2021; Nigam & Kumar, 2022; Sunkari et al., 2022).

The Northern Region of Ghana is acknowledged for its restricted access to quality freshwater supplies (Jeil et al., 2020). Recent statistics from 2021 show that approximately 21 percent of households in this area lack improved access to freshwater supplies (Ghana Statistical Service [GSS], 2022; Erga, 2023). This scarcity of water availability in semi-urban and rural areas forces local populations to resort to using water from unsecured surface reservoirs (Erga, 2023; Community Water and Sanitation Agency [CWSA], 2023). As a result, factors like increasing temperatures, urban growth, and increasing population exacerbate the strain on water resources, particularly in the northern part of Ghana, leading to widespread reliance on the use of contaminated water (Agodzo et al., 2023). Thus, groundwater reliance remains crucial for rural communities in Ghana's Northern Region known as one of the country's driest regions, serving various purposes from household use to minor agricultural and industrial activities (Asare-Donkor and Adimado, 2020; Chegbele et al., 2020). However, challenges arise, such as boreholes drying out due to over-pumping, compounded by inadequate enforcement of groundwater management laws (Cobbina et al., 2012; Walker, 2022).

While much attention has been directed towards ensuring sustainable extraction of groundwater resources, it is equally imperative to conduct a comprehensive assessment of the factors influencing water quality from the aquifers underlying the region's aquifers. This is crucial as high-quality groundwater is essential for long-term irrigation and domestic purposes. Saline concentration of groundwater has been of significant concern, which plays a pivotal role in determining its suitability for irrigation, as high salinity levels can adversely affect soil quality.

Therefore, a comprehensive assessment of the standard of groundwater supplies provided by this extensive region is highly essential within the broader assessment of the groundwater supply foundation of the region.

Traditional approaches have been utilized to analyze the appropriateness of groundwater for agricultural need within the region. In fact, Ghana has a long history of employing multivariate analysis methods to examine water quality parameters (Banoeng-Yakubo et al., 2009; Loh et al. 2016; Chegbele et al. 2020; Obiri-Nyarko et al., 2022).

In Ghana, groundwater research has made extensive use of geostatistical approaches. For example, research by Loh et al. (2020) examined the chemistry of groundwater in several areas of the Savannah Region of Ghana such as the Sawla-Tuna-Kalba District. They utilized multivariate statistical methods and hydrochemical plots to analyze 112 samples, revealing the dissolving of silicate minerals and the impact of agricultural chemicals and household wastewater as primary causes of hydrochemical differences within the research region. Similarly, Chegbele et al. (2020) performed a thorough assessment of the chemical composition of groundwater in the Talensi area through traditional graphical

approaches and multivariate statistical methods. Their research identified three main flow regimes through the Q-mode clustering technique, revealing mixed cation-based water categories. Numerous additional comparable research in Ghana have been extensively recorded by researchers such as Yidana (2011), Loh et al. (2016), Dorleku et al. (2016), and Sunkari et al. (2022).

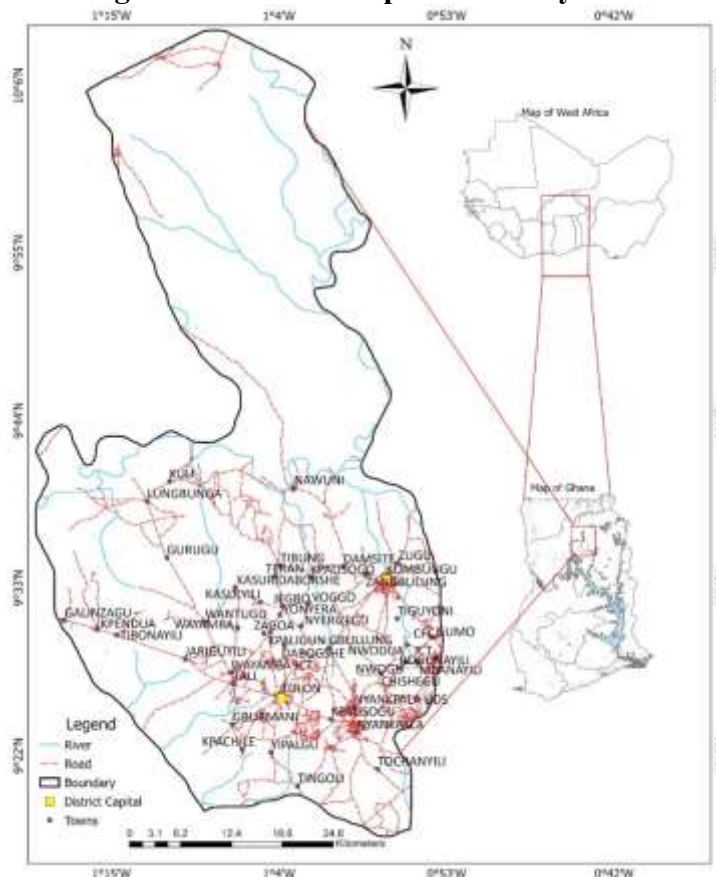
This research employs multivariate statistical techniques and geographic information system to examine the key variables influencing groundwater condition and its appropriateness for agricultural and household uses in selected areas of the Tolon-Kumbungu area.

## 2 Study Area

### 2.1 Location, Topography, Drainage and Climate

The research location (Figure 1) is situated within the Northern Region of Ghana. Geographically, it spans between latitudes 9° 17' N and 10° 06' N, and longitudes 0° 55' W and 1° 21' W (Mumuni and Bayor, 2017), surrounded to the north by the West Mamprusi District, to the west by the West Gonja District, to the south by the Central Gonja District, and to the east and southeast in that order by the Savelugu-Nanton District and the Tamale Metropolitan area (Abagale et al., 2020; Erga, 2023)

**Figure 1 Location Map of the Study Area**



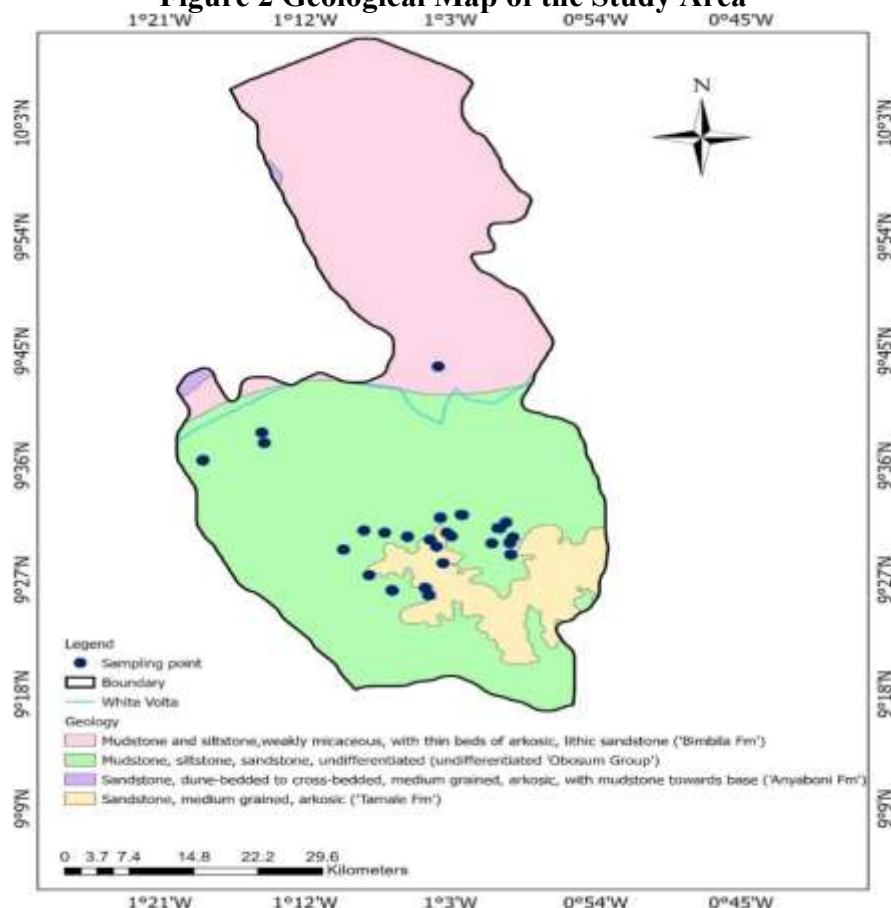
Topographically, the land has rolling terrain with scattered depressions, lacking significant high elevations throughout the district (Cobbina et al., 2012; Abdul-Ganiyu et al., 2017; Abagale et al., 2020). Drainage is facilitated by several rivers and streams, with the White Volta being the most prominent. These water bodies exhibit dendritic drainage patterns (Cobbina et al., 2012; Ghana Statistical Service, 2014; Abdul-

Ganiyu et al., 2017). The climate is marked by a singular rainy season, commencing in late April with minimal rainfall, peaking in July-August, and tapering off abruptly by October-November (Abagale et al., 2020). The dry season spans from November to March, with daytime temperatures that range from 33°C to 39°C and nighttime temperatures averaging between 20°C and 26°C. Annual rainfall typically falls within the range of 950mm to 1,200mm. Humidity levels during April to October peak at around 95% during the night, diminishing to 70% during the day, while for the remainder of the year, nighttime humidity ranges from 80% to 25%. Soil composition predominantly consists of sandy loam, with alluvial deposits present in low-lying areas (Ghana Statistical Service, 2014). Additionally, there are gravel deposits exploited for economic purposes. The soil's composition renders it susceptible to erosion, particularly sheet and gully erosion.

## 2.2 Geology and Hydrogeology

The research area falls within the geological confines of the Voltaian Sedimentary Basin, characterized by a diverse range of rock formations including fine-grained sandstone, mudstone, shale, siltstone, and occasional intercalations of these materials (Cobbina et al., 2012; Mumuni and Bayor, 2017; Abagale et al., 2020). Within this basin, the Middle Voltaian Palaeozoic rocks, comprising shale, mudstone, sandstone, limestone, and conglomerate, constitute the basement rocks underlying the region (Cobbina et al., 2012; Mumuni and Bayor, 2017; Abagale et al., 2020). A minor part of the area, situated in the far northwest, is underlain by Upper Voltaian sandstone and quartzite (Figure 2). Shale predominantly forms the bedrock across the area, with varying groundwater potential influenced by climatic conditions and geological factors (Cobbina et al., 2012).

**Figure 2 Geological Map of the Study Area**



Hydrogeologically, the Palaeozoic Voltaian sedimentary rocks exhibit characteristics akin to hard rocks. Although the sandstones are relatively impermeable, they contain fissures along joints, fractures, bedding, and cleavage planes, allowing for the percolation of water into the underlying regolith to form groundwater reservoirs (Cobbina et al., 2012; Mumuni and Bayor, 2017; Abagale et al., 2020). Groundwater primarily derives from the weathered layer or regolith atop the rocks, as well as fractures within the bedrock (Cobbina et al., 2012; Abagale et al., 2020). The aquifers exhibit a phreatic to semi-confined nature, often being structurally dependent and sporadic in occurrence. The presence of lateritic cover diminishes groundwater potential in shale-rich areas, while regions underlain by mudstones typically exhibit impermeability (Cobbina et al., 2012). Water extraction primarily occurs from wells situated in fractured zones with saturated regolith, rather than from extensive aquifers. Borehole depths recorded by Cobbina et al., 2012 ranged from 25 to 96 meters, with an average depth of 43 meters.

### 3 Methodology

The study utilized secondary data obtained from the Water Research Institute of the Council for Scientific and Industrial Research (CSIR-WRI). The dataset consisted of 46 groundwater samples obtained from boreholes and hand-dug wells equipped with pumps, which were analyzed for major and minor ions. It was observed that; samples were collected in sterilized 250-ml polythene bottles and stored in cool boxes at approximately 3°C during transportation to the CSIR-WRI laboratory for analysis of major and trace cations and anions. Field measurements, such as electrical conductivity (EC), temperature (T), and pH values, were recorded as part of the dataset, focusing on parameters prone to change during transport. Observations during data acquisition suggest that standard water sampling and storage protocols prescribed by the US Geological Survey (USGS, 2019) were followed during the original data collection. Data collected underwent consistency tests using the charge balance error (CBE) approach:

$$CBE = \frac{\sum z.m_c - \sum z.m_a}{\sum z.m_c + \sum z.m_a} \times 100 \quad (1)$$

Where the concentrations of the ions are in milliequivalents per liter. In this formula, z signifies the magnitude of an ion's charge, while mc and ma represent the molar concentrations of cations and anions, respectively. The charge balance error calculation considered major concentrations including  $Na^+$ ,  $Mg^{2+}$ ,  $Ca^{2+}$ ,  $K^+$ ,  $Cl^-$ ,  $HCO_3^-$ ,  $PO_4^{3-}$ , and  $NO_3^-$  for each sampling period. Samples deviating beyond the acceptable limit of  $\pm 5\%$  were excluded from further analysis, resulting in 41 samples. Major Ion Balance Analysis serves as a crucial aspect of quality control in chemical analysis.

The parameters underwent a normality test, revealing that none of them met the criteria suitable for effective multivariate statistical evaluation. Consequently, all parameters underwent logarithmic transformation to normalize the data. Standardization was then applied to homogenize the data to their respective z-scores.

$$z = \frac{x - \mu}{s} \quad (2)$$

Where x,  $\mu$ , and s correspond to the parameter's value, the average, and the data's standard deviation. Hierarchical cluster analysis (HCA) was subsequently employed on the standardized z-scores. Cluster analysis (CA) is a multivariate statistical technique that organizes parameters or variables into categories based on perceived similarities or dissimilarities (Yidana et al., 2020). Among the methods of cluster analysis, HCA is the most commonly utilized one, dividing data into levels according to their similarity or dissimilarity (Yidana et al., 2010; Aljumily, 2016). Q-mode HCA was employed to the data. Q-mode HCA, a variant of hierarchical cluster analysis, groups samples into clusters to provide insights into the



development and transformation of surface and groundwater systems and to distinguish hydrochemical facies. Parameters were initially classified into clusters using square Euclidean distances, with the Ward's linkage approach employed to connect resultant initial clusters. This integration of dissimilarity measure and linkage approach is noted to produce the best outcomes in hierarchical cluster analysis (Chegbeleh et al., 2020; Loh et al., 2020).

R-mode factor analysis was conducted by selecting principal components and employing varimax rotation. R-mode factor analysis involves the grouping of parameters, with principal component analysis (PCA) being a commonly used extraction method. Principal Component Analysis serves as a method to minimize dimensions by identifying key elements or features, aiding in the interpretation of an extensive dataset and visualizing relationships among different parameters, potentially reducing the quantity of parameters. Principal Component Analysis was carried out using the correlation matrix, with data normalized to a uniform scale, and principal components arranged in descending sequence of variance, prioritizing the most impactful components first (Yidana et al., 2010, 2012; Chegbeleh et al., 2020; Loh et al., 2020).

The relationships and mechanisms influencing hydrochemistry, inferred from advanced statistical methods, were reinforced through the use of traditional chemical plotting tools and stability charts. These resources helped determine the key factors affecting groundwater composition and pinpoint the most stable mineral forms within the groundwater flow system.

Groundwater quality was further evaluated regarding its suitability for consumption and agricultural use using a water quality index (WQI) approach, adapted from Brown et al. (1972), and weighted for parameters relevant to domestic water quality analysis. The WQI computation involved a four-step process.

Initially, the parameters ( $K^+$ ,  $Cl^-$ ,  $PO_4^{2-}$ ,  $NO_3^-$ ,  $Na^+$ ,  $Mg^{2+}$ ,  $Ca^{2+}$ ,  $F^-$ , TDS, As, Mn, Fe, TH and pH) in groundwater were assigned weights according to their relative importance within potable water guidelines, with critical factors such as  $F^-$ ,  $NO_3^-$ , and As assigned the maximum weight of 5. Other parameters ( $K^+$ ,  $Cl^-$ ,  $PO_4^{2-}$ ,  $SO_4^{2-}$ ,  $Na^+$ ,  $Mg^{2+}$ ,  $Ca^{2+}$ , TDS, Mn, Fe and pH) were allocated weight values ranging from 1 to 4 determined by their significance. Next, the relative weight ( $W_i$ ) for each parameter was calculated (Equation (3)),

$$W_i = \frac{w_i}{\sum_{i=1}^n w_i} \quad (3)$$

Where,  $W_i$  is the relative weight,  $w_i$  = weight of individual parameters and  $n$  = number of parameters.

The next step involves assigning a quality rating scale ( $q_i$ ) corresponding to every parameter, based on its level relative to WHO drinking water standards using equation 4.

$$q_i = \frac{C_i}{S_i} \times 100 \quad (4)$$

where,  $q_i$  represents the quality rating,  $C_i$  denotes the concentration of each chemical parameter in individual groundwater samples (mg/L), and  $S_i$  refers to the corresponding WHO drinking water standard (mg/L).

Subsequently, the WQI was calculated using the specified equation.

$$SI_i = q_i \times W_i \quad (5)$$

$$WQI = \sum SI_i \quad (6)$$

Where,  $SI_i$  is the sub-index of the  $i$ th parameter. The weights and relative weights of the parameters were determined based on WHO (2017) standards. The assigned weight ( $w_i$ ) and relative weights ( $W_i$ ) for the

parameters are shown in Table 1 following the framework outlined by Sahu and Sikdar (2008) depicted in Table 2.

**Table 1 Relative Weights for the Parameters**

Parameter-mg/L	WHO standards	Weights	Relative weights
Na <sup>+</sup>	200	2	0.0385
TH	200	4	0.0769
Ca <sup>+</sup>	200	2	0.0385
Mg <sup>+</sup>	150	2	0.0385
K <sup>+</sup>	30	2	0.0385
TDS	500	4	0.0769
pH	6.5-7.5	4	0.0769
NO <sub>3</sub> <sup>-</sup>	10	5	0.0962
F <sup>-</sup>	1.5	5	0.0962
PO <sub>4</sub> <sup>-</sup>	0.7	4	0.0769
Cl <sup>-</sup>	250	3	0.0577
As	0.01	5	0.0962
Fe	0.3	3	0.0577
Mn	0.4	4	0.0769
SO <sub>4</sub> <sup>2-</sup>	250	3	0.0577
		$\sum w_i = 52$	$\sum W_i = 1.00$

**Table 2 Water Quality Ratings**

WQI	Description
<50	Excellent
50-100	Good
100-200	Poor
200-300	Very Poor
>300	Unfit for drinking

ArcGIS Pro 2.8.0, a geospatial information software, was employed to generate a Water Quality Index (WQI) map using the inverse distance weighting approach. To reduce inaccuracies linked to spatial estimation, all interpolations were limited to locations within the research area having a well-distributed arrangement of sample points, excluding regions lacking any sampling data.

For assessing groundwater suitability for irrigation, the Wilcox (1955) diagram was utilized. Wilcox (1955) plot of sodium percentage against EC was employed to classify water types into various clusters suitable for irrigation. Elevated sodium levels impede mineral particle and nutrient mobility and reduce water penetration. Sodium percentage (Na%) of water samples, calculated as the ratio of sodium to the sum of major cations, was used to determine the Na% of each sample.

$$\text{Na\%} = \frac{\text{Na}}{\text{Na} + \text{Ca} + \text{Mg} + \text{K}} \times 100 \quad (7) \text{ where concentrations are expressed in milliequivalents per liter.}$$

## 4 Results and discussions

### 4.1 Summary Statistics of Hydrochemical Data

A statistical summary of the hydrochemical data is presented in Table 3, revealing considerable variance in most major chemical parameters. This variability indicates diverse sources and influences impacting groundwater concentrations across the research area. Generally, the average values for the measured parameters are within the permissible thresholds defined by the World Health Organization (WHO, 2017) for both domestic and irrigation needs.

**Table 3 Overview of Key Physicochemical Parameters Utilized in the Study**

Parameters	Average	SD	Min	Max
pH	7.79	0.53	6.75	8.58
EC	1452.57	1393.55	83.4	5850.00
TDS	726.83	697.64	41.70	2930.00
Total Hardness	114.15	59.06	36.0	264.00
Alkalinity	169.35	77.72	50.00	324.00
Ca <sup>2+</sup>	27.95	17.94	5.60	75.40
Mg <sup>2+</sup>	11.05	4.78	3.40	30.10
Na <sup>+</sup>	212.62	226.26	16.10	968.00
K <sup>+</sup>	1.98	0.63	0.90	3.80
HCO <sub>3</sub> <sup>-</sup>	202.72	96.57	8.50	395.00
SO <sub>4</sub> <sup>2-</sup>	45.68	49.48	4.0	254.00
Cl <sup>-</sup>	240.08	400.56	7.0	1666.00
NO <sub>3</sub> <sup>-</sup>	0.23	0.41	<0.01	1.93
PO <sub>4</sub> <sup>-</sup>	0.15	0.18	<0.01	0.58
F	0.72	0.47	0.1	2.00
Fe	0.06	0.08	<0.01	0.45
Mn	0.04	0.06	<0.01	0.31
SiO <sub>2</sub>	29.14	18.17	12.30	76.70
As	0.01	0.01	<0.01	0.03

However, there are instances where concentrations of certain parameters exceed acceptable levels for domestic water supply. Groundwater pH is particularly important in influencing mineral dissolution within aquifers, subsequently impacting water quality for various uses (Chegbeleh et al., 2020; Ram et al., 2021; Snousy et al., 2022). In the district examined, the pH shows only slight fluctuations, spanning from 6.75 to 8.58, with a mean of 7.79 and a standard deviation of 0.53. This range categorizes the groundwater as mildly alkaline, consistent with the natural water pH interval of 6.5 to 8.5 as advised by the World Health Organization (WHO, 2017). In contrast, electrical conductivity (EC) and total dissolved solids (TDS) exhibit significant variation across the district. The highest EC levels are observed in Tanshegu and Voggu, located in the southeast and central portion of the research location, respectively, with an average EC of 1452.57  $\mu$ S/cm and a range of 38.4 to 5850  $\mu$ S/cm. Lower EC values are found in the northeastern



regions. This variation suggests some degree of groundwater mineralization, influenced by geological factors and varying anthropogenic impacts across the area (Cobbina et al., 2012). TDS values associated with these EC values span from  $41.70 \text{ mgL}^{-1}$  to  $2930.00 \text{ mgL}^{-1}$ , with a mean of  $726.83 \text{ mgL}^{-1}$ . The elevated maximum values indicate the occurrence of saline or mineral-rich water sources in certain locations, particularly in Tanshegu and Voggu, where concentrations exceed  $1000 \text{ mg/L}$  (Lee et al., 2021; Krishna and Achari, 2024). As precipitation percolates through soil and rock layers, it dissolves minerals, carrying dissolved particles along the way (Mather, 2020; Chegbeleh et al., 2020). Such elevated TDS levels may pose health risks if untreated water is consumed (Wang, 2021; Luvhimbi et al., 2022; Sangwan et al., 2022) and could also negatively impact agriculture and soil quality in these regions (Dhaouadi et al., 2020; Samaei et al., 2022).

Total hardness levels range from  $36 \text{ mg/L}$  in Lungbunga and Tali to  $264 \text{ mg/L}$  in Tanshegu, indicating moderate to high water hardness across sampled areas. Higher hardness in communities like Tanshegu and Vawagiri-Tolon may be influenced by local geological features that increase mineral dissolution (Gao et al., 2021; Qureshi et al., 2021). Hard water consumption is generally safe, even beneficial, as it provides essential minerals like calcium and magnesium, supporting dietary needs (Chegbeleh et al., 2020).

Calcium and magnesium are crucial indicators of groundwater quality, revealing geological characteristics and potential health impacts for dependent communities (Aragaw and Gnanachandrasamy, 2021). In the Tolon-Kumbungu District, calcium concentrations varied significantly, with a mean of  $27.95 \text{ mgL}^{-1}$ . The highest calcium level,  $75.4 \text{ mgL}^{-1}$ , was observed in Tanshegu, while Tali had the lowest at  $5.6 \text{ mgL}^{-1}$ , all within the acceptable WHO thresholds. Magnesium levels also showed variation, averaging  $11.05 \text{ mgL}^{-1}$ , with the maximum concentration of  $30.1 \text{ mgL}^{-1}$  recorded in Wantugu and the minimum of  $3.4 \text{ mgL}^{-1}$  in Lungbunga. These results confirm that calcium and magnesium concentrations remain well within WHO safety thresholds, suggesting that groundwater in this district is generally suitable for consumption.

Notably, while sodium levels are considered suitable for drinking, average concentrations of Na surpass  $200 \text{ mg/L}$  in some locations. Approximately 20% of the sampled locations presented sodium concentrations above this limit. Elevated levels of sodium may arise from various factors such as the dissolution of soluble salts like halite, or through ion exchange processes (Chegbeleh et al., 2020). High sodium intake is linked to health issues like hypertension and hardening of the arteries, while insufficient intake can lead to dehydration and sensory impairments (Kokkat et al., 2016; Aragaw and Gnanachandrasamy, 2021).

In contrast, potassium concentrations remained relatively stable across the sampled towns, with a mean of  $1.98 \text{ mgL}^{-1}$ . The maximum value was observed at  $3.8 \text{ mg/L}$  in Cheshegu, while the minimum was recorded at  $0.9 \text{ mg/L}$  in Munya. Notably, all potassium levels in the sampled groundwater fell below the WHO threshold of  $12 \text{ mgL}^{-1}$ , indicating that potassium levels are generally within safe limits for human consumption.

The average bicarbonate concentration across all samples was approximately  $202.72 \text{ mg/L}$ , with a remarkable maximum concentration of  $395 \text{ mg/L}$  recorded in both Cheshegu and Jegbo, while the minimum was notably low at  $8.5 \text{ mg/L}$  in Shedua. Bicarbonate levels above  $100 \text{ mg/L}$  are generally considered indicative of good groundwater quality, and the majority of the samples in this study fell well within this range. However, the high concentrations observed in some towns indicate a significant presence of bicarbonate, which may be attributed to the dominance of mineral dissolution in the region or the influence of organic matter decomposition (Loh et al., 2016; Chegbeleh et al., 2020; Aragaw and Gnanachandrasamy, 2021; Sankoh, 2022).

The average chloride concentration across the sampled towns was calculated to be  $240.0 \text{ mgL}^{-1}$ , with a maximum level of  $1,666 \text{ mgL}^{-1}$  recorded in Voggu, significantly exceeding the World Health Organization (WHO) guideline limit. Elevated chloride ion levels indicate potential anthropogenic influences, likely stemming from agricultural activities and the persistent use of fertilizers and chemicals in the region (Loh et al., 2016; Chegbele et al., 2020; Ren and Zhang, 2020; Aragaw and Gnanachandrasamy, 2021; Çadraku, 2021; Wali et al., 2022). Such chemicals can infiltrate and seep into the groundwater system over time, leading to heightened  $\text{Cl}^-$  concentrations. The fluoride levels varied between a lowest value of  $0.1 \text{ mgL}^{-1}$ , observed in several locations such as Gbullung and Jegbo, to a maximum of  $2.0 \text{ mg/L}$  recorded in Voggu. The average concentration across the sampled towns was  $0.72 \text{ mg/L}$ . A notable trend emerged where towns with elevated fluoride concentrations also exhibited higher chloride levels. For instance, Voggu not only had the highest chloride concentration but further showed a fluoride level of  $2.0 \text{ mgL}^{-1}$ , exceeding the WHO guideline of  $1.5 \text{ mgL}^{-1}$ . The increased fluoride levels detected in certain sections of the Voggu community within the research region could be linked to the leached and weathered fluorite or the effect of alkaline water nearby (Cobbina et al., 2012; Hossain and Patra, 2020; Mukherjee and Singh, 2020; Yadav et al., 2021; Chaudhuri et al., 2024). According to Viero et al. (2009), alkaline waters may prevent fluoride from being adsorbed onto clay mineral surfaces.

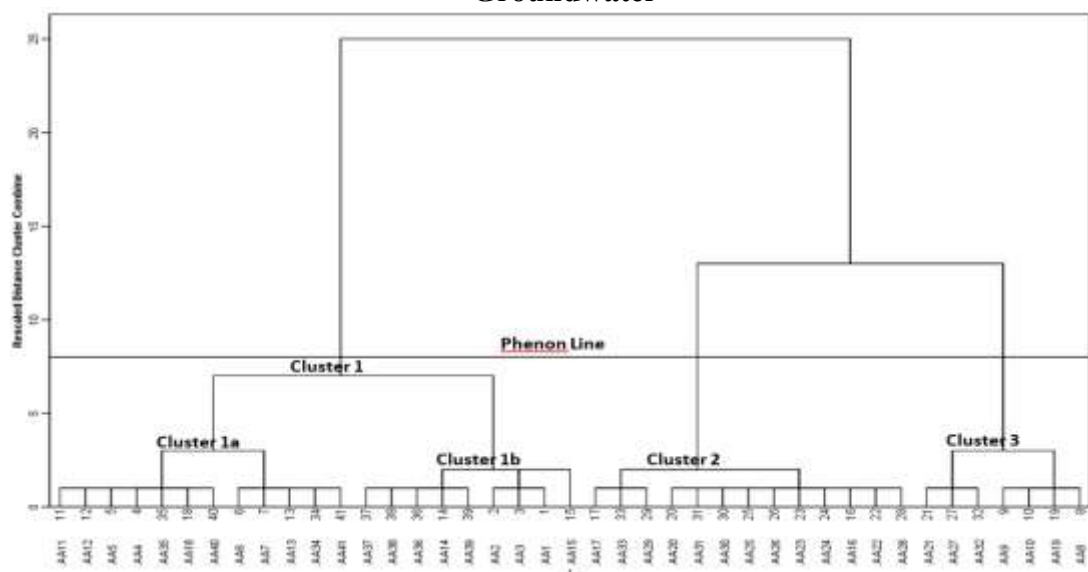
The average concentration of iron was calculated to be  $0.06 \text{ mgL}^{-1}$ , with a highest value of  $0.45 \text{ mgL}^{-1}$  recorded at Tali and a lowest of  $0.008 \text{ mgL}^{-1}$  at Gbullung. Notably, the majority of samples, except for a few, remained well within the WHO guideline limit of  $0.3 \text{ mg/L}$ . The Fe measurements account for the total concentration, including particles in the water, rather than just the dissolved iron levels, which are determined after filtering the samples. The high value could be as a result of the weathering and dissolution of iron-rich minerals and the possible influence of human activities like agriculture (Cobbina et al., 2012; Ram et al., 2021).

Parameters such as sulphate ( $\text{SO}_4$ ), nitrate ( $\text{NO}_3$ ), phosphate ( $\text{PO}_4$ ), and manganese (Mn) all fell within the World Health Organization (WHO) limits, indicating that the concentrations of these elements in the sampled groundwater do not present any health risks based on the 2017 guidelines.

#### 4.2 Definition of recharge and discharge zones

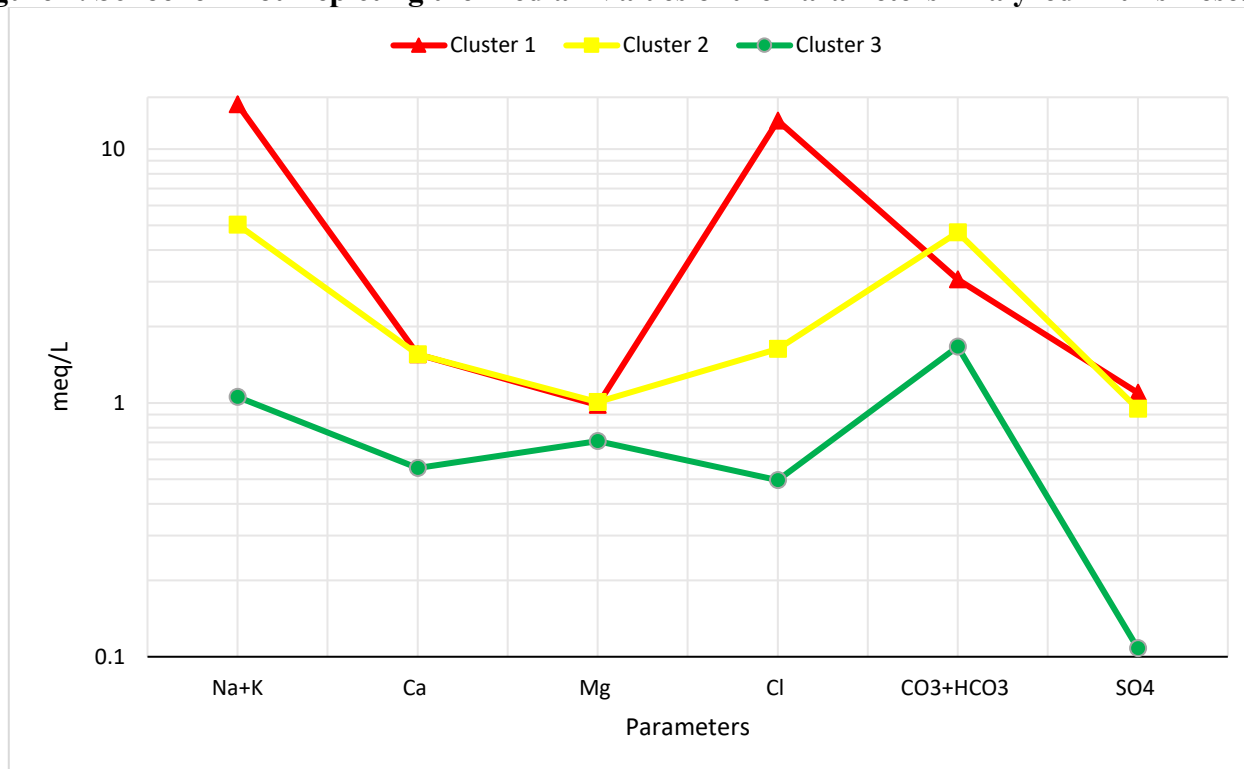
The results of the Q-mode hierarchical cluster analysis were represented through a dendrogram (Figure 3), providing a graphical representation of the grouping generated through the analysis. A phenon line was drawn on the dendrogram at approximately 8 units. This placement of the phenon line aims to strike a balance, ensuring that neither an excessive nor inadequate number of clusters are generated, as this could complicate interpretation or overlook important hydrochemical processes. The grouping derived from the dendrogram is interpretative and guided by the researcher's knowledge of various aspects of the environment, like geological formations, hydrological characteristics, and anthropogenic influences within the study region, all of which can affect groundwater chemistry. The results of the clustering process divide the region of study into three separate groups.

**Figure 3. Dendrogram From The Q-Mode HCA Illustrating the Spatial Relationships of Groundwater**



Schoeller and Stiff diagrams (Figures 4 and 5) were produced by averaging the hydrochemical characteristics from the three clusters. This improved the depiction of the principal hydrochemical characteristics of the area and potential factors influencing groundwater composition. Despite this, the three clusters exhibit distinct variations in ionic concentrations, indicating different patterns within the groundwater system. Figure 4 highlights that, cluster 1 displays the most elevated levels of key chemical components across the study region. Notably, cluster 1 is associated with lower median altitudes and the highest electrical conductivity (EC), primarily located in areas with lower elevations like Voggu. Cluster 2, situated between clusters 1 and 3, represents a transitional zone. In recharge areas, groundwater typically exhibits low ion concentrations akin to local precipitation. However, as water moves through the subsurface, dissolving geological materials and various substances, the concentration of ions in the water becomes higher, which explains the reason clusters 3 and 1 correspond to recharge and discharge zones, respectively, while cluster 2 samples represent a transitional phase between these zones.

**Figure 4. Schoeller Plot Depicting the Median Values of the Parameters Analyzed in this Research**

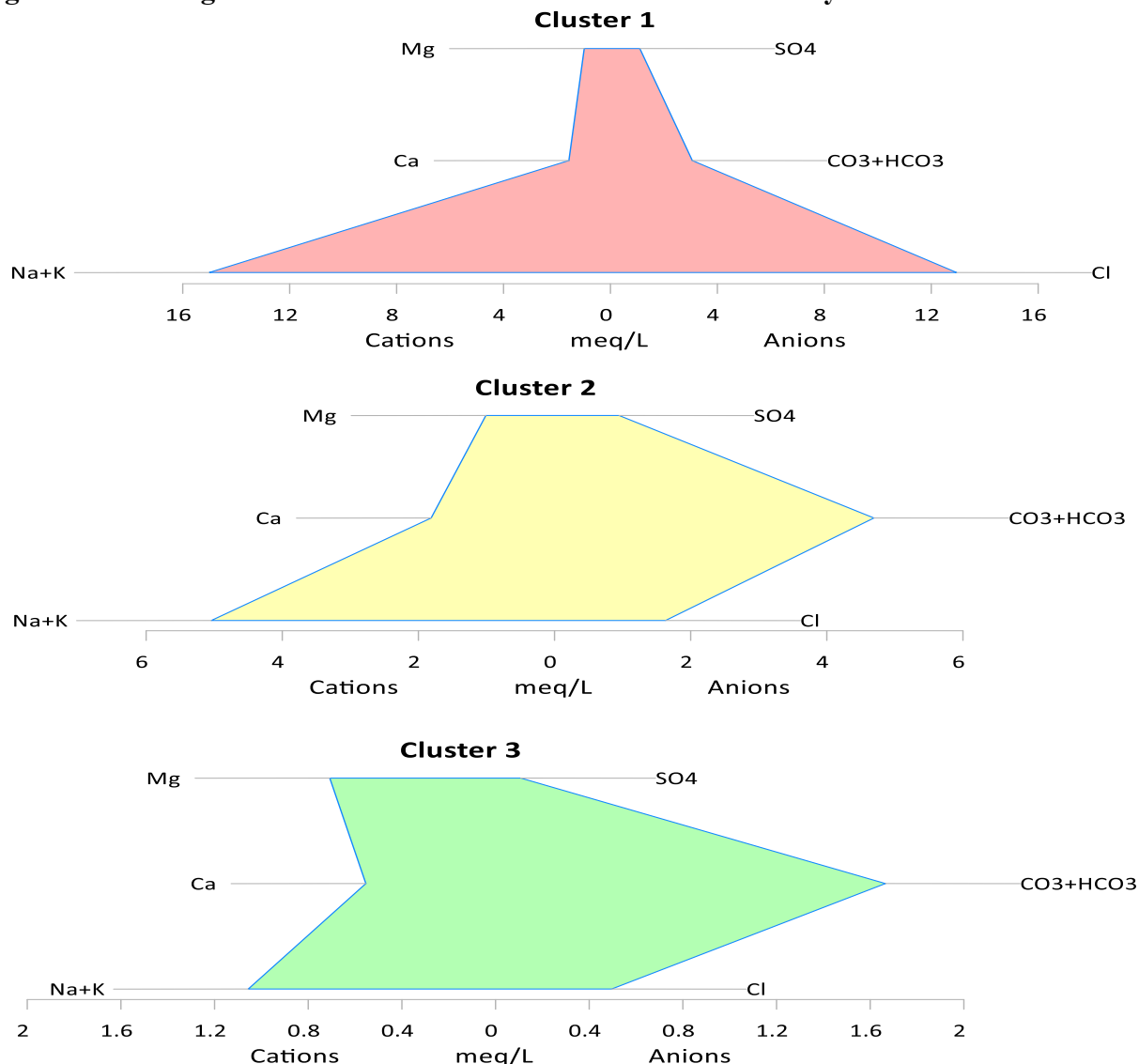


The Stiff diagrams in Figure 5 vividly illustrate these dynamics. Cluster 3 depicts a fresh water type characterized by the presence of Na + K-Mg-HCO<sub>3</sub> in the groundwater flow system, accompanied by a mean pH that is comparatively low at 6.91. This pH level may stem from CO<sub>3</sub><sup>2-</sup> reacting with precipitation to form carbonic acid, or from CO<sub>3</sub><sup>2-</sup> released into the groundwater system through plant cellular respiration. Cluster 3 comprises samples primarily from the communities Gingani, Tali, Shedua, Bungnaayili, and Kpaligun, that are located in proximity and characterized by sandstones, and other formations. Additionally, Cluster 3 exhibits weakly mineralized groundwater, indicated by lower major ion concentrations, typical of recharge zones. This could be due to rapid preferential recharge through macropores or short residence times in the geological material. The low pH conditions in Cluster 3 foster favorable conditions for rock mineral weathering, liberating ions like Na<sup>+</sup>, Mg<sup>2+</sup> and Ca<sup>2+</sup> into solution from the district's predominant silicate and carbonate minerals.

In contrast, subsequent groupings reveal a trend of escalating mineral content, with Cluster 2 (Na-HCO<sub>3</sub><sup>-</sup> type) representing a transitional water type showing a moderate level of mineralization, while Cluster 1 (Na-Cl type), indicative of discharge areas, exhibits a notably higher mineral content (Figure 4). This implies extended periods of water residence and increased interactions between groundwater and rock formations as water traverses from recharge to discharge regions.

The overall concentration of dissolved ions appears to rise during the progression of groundwater from a Na + K-Mg-HCO<sub>3</sub> dominant fresh water type in Cluster 3 (recognized as a recharge zone) to a Na-Cl water type in Cluster 1 (identified as a discharge zone). Clusters 2 and 3 have average pH values of 7.66 and 8.10 respectively. Cluster 1 predominantly comprises samples from Gung, Voggu, Munya, Gbullung, and Gbanjogla, locations characterized by moderate to lower elevations within the region, hence identified as discharge zones.

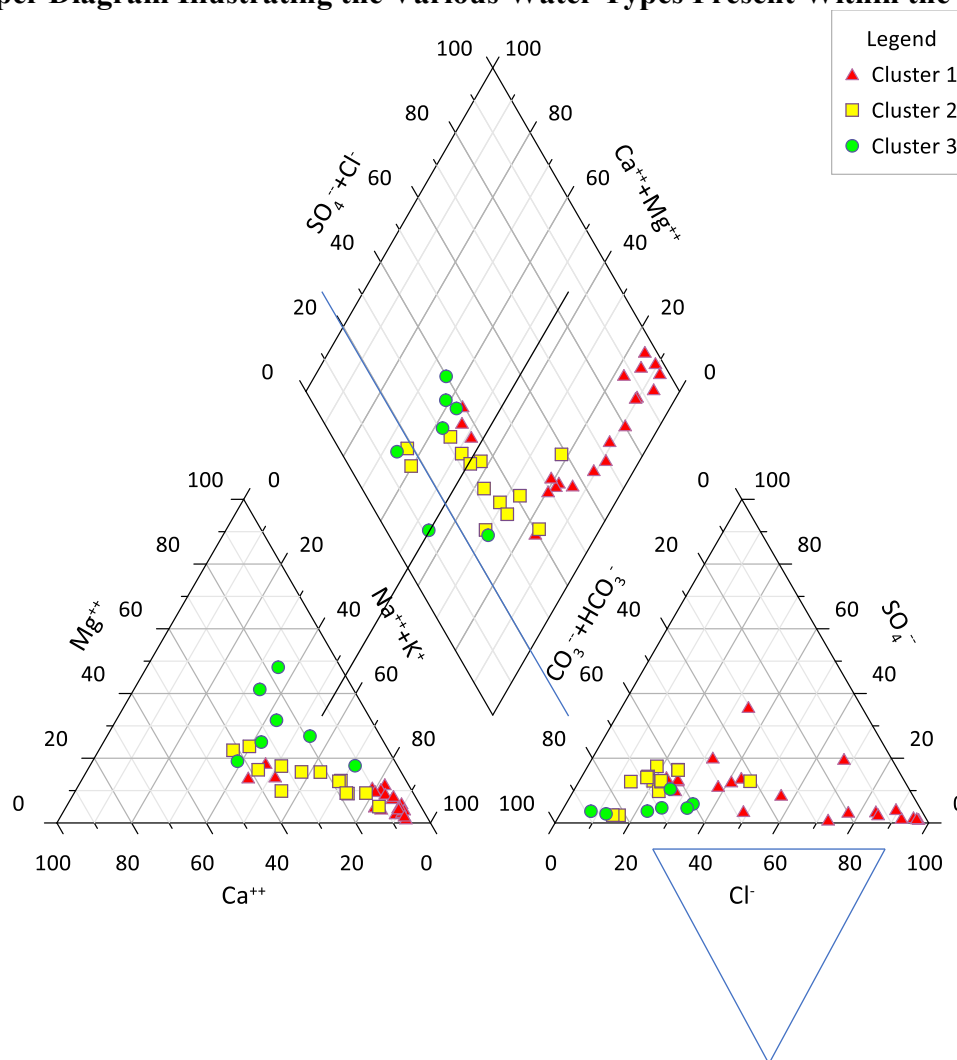
**Figure 5 Stiff Diagrams Based on The Mean Concentrations of Key Ions in the 3 Clusters**



Further insights into the hydrochemistry of the district are gained through the creation of Piper (1944) and Durov (1948) diagrams. While both diagrams provide valuable information, the Durov (1948) diagram offers additional advantages by elucidating hydrochemical processes influencing groundwater formation alongside water classification. Figure 6 illustrates that the majority of groundwater samples are characterized by Na cation dominance, suggesting the prevalence of alkali earth over alkaline elements (thus  $\text{Na}^+ + \text{K}^+ > \text{Mg}^{2+} + \text{Ca}^{2+}$ ). The piper diagram reveals Cluster 1 is more enriched in Na than Cluster 2 and 3. Three categories of water are distinguishable: Na-Cl water type having 17 samples, Ca-Na-HCO<sub>3</sub> type with 14 samples and Ca- HCO<sub>3</sub> with 10 samples. Cluster 1 aligns more closely with the Na-Cl water type, while Cluster 2 and 3 exhibit closer associations with Ca-Na-HCO<sub>3</sub> and Ca-HCO<sub>3</sub> types respectively. The analysis indicates a prevalence of weak acids over strong acids in the groundwater samples from the research region. This observation suggests an evolutionary trend wherein water types initially dominated by Ca-HCO<sub>3</sub>, typical of recharge regions, transition to Ca-Na-HCO<sub>3</sub> types resulting from reverse cation exchange mechanisms within the aquifer system.

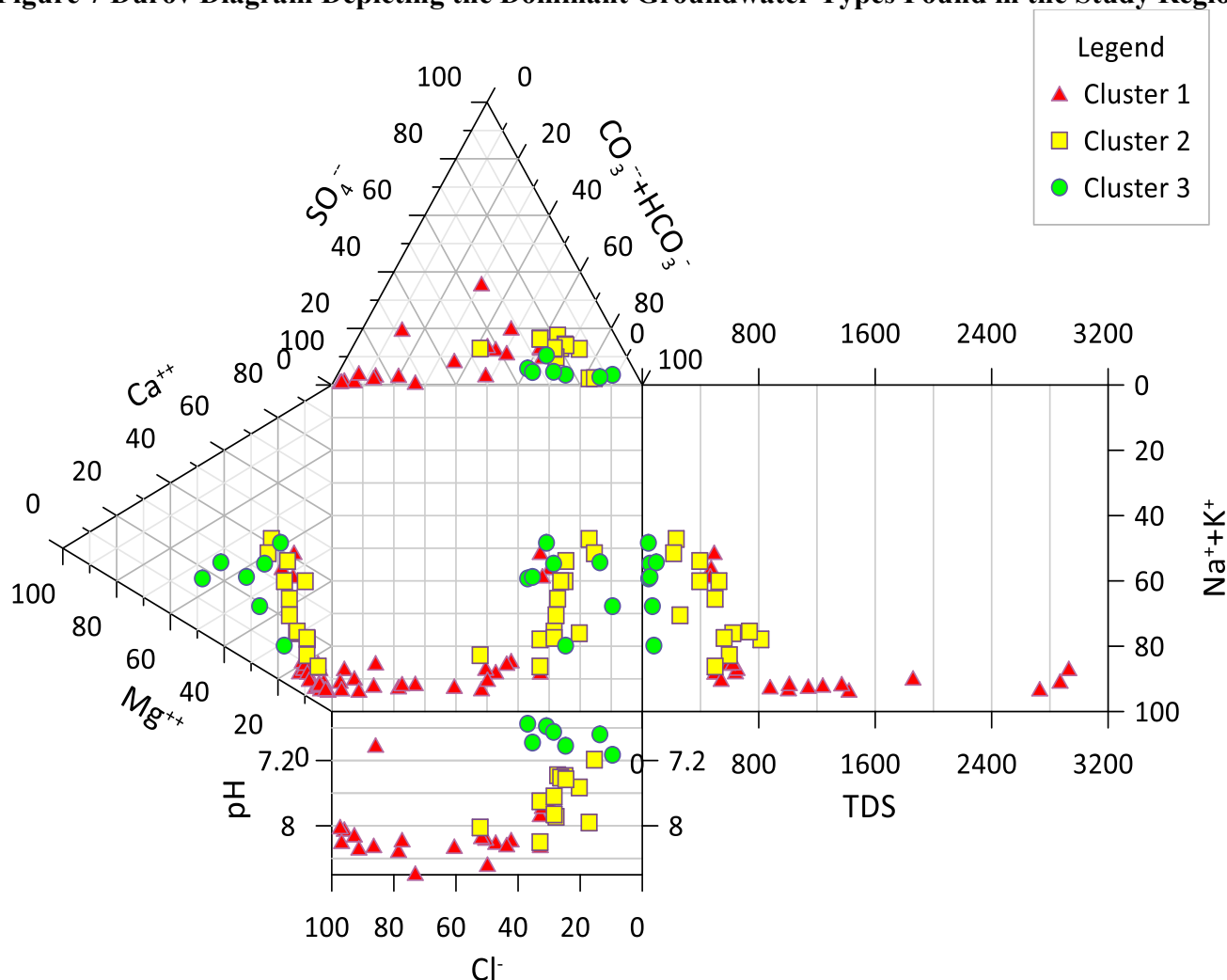


**Figure 6 Piper Diagram Illustrating the Various Water Types Present Within the Study Region**



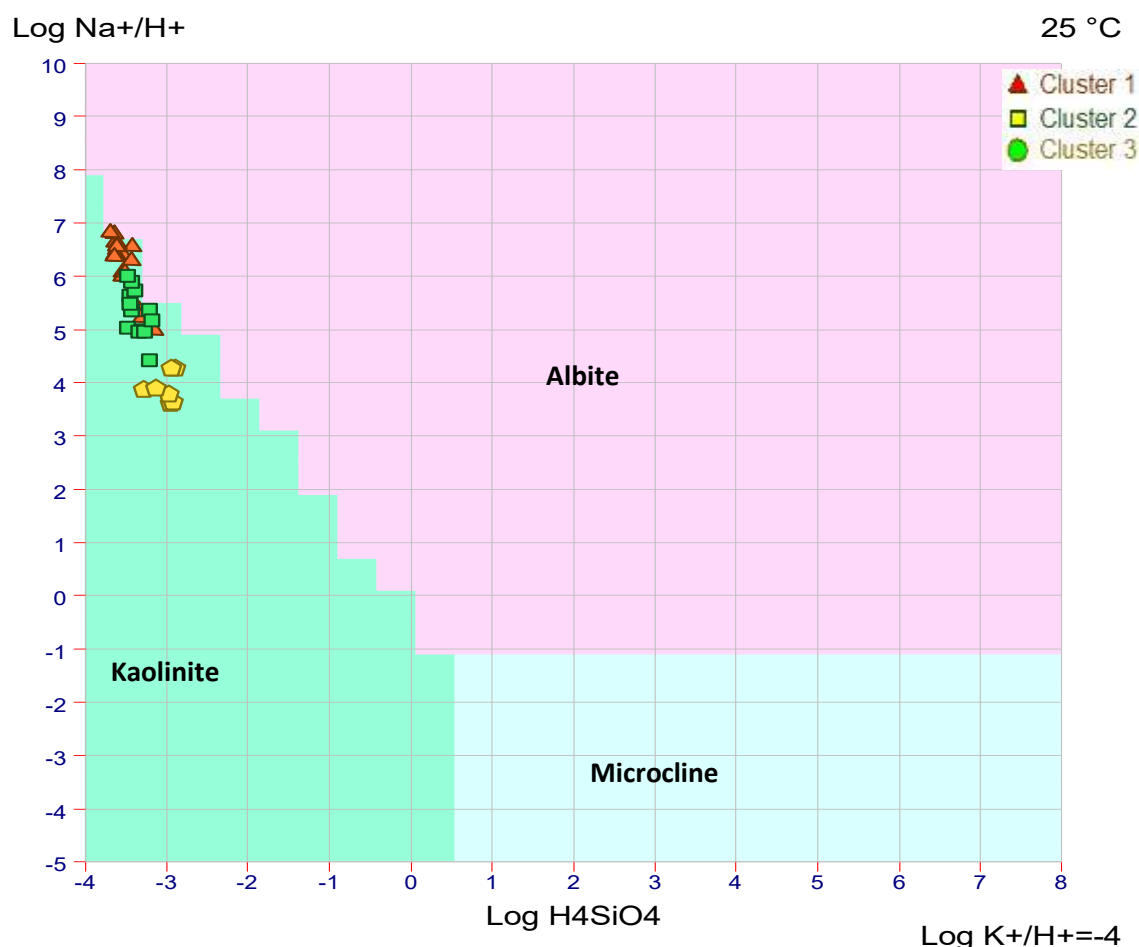
The Durov plot depicted in Figure 7 mirrors the hydrochemical trends observed in the Piper plot, with a notable skew towards Na dominance among the samples. It suggests that two primary hydrochemical processes, namely simple dissolution and reverse ion exchange, influence groundwater chemistry within the research area. The occurrence of reverse ion exchange might be attributed to the dissolution of phyllosilicates like micas and clay minerals, prevalent constituents of the local geological makeup (as depicted in Figure 2). This process likely leads to the replacement of alkaline earth elements with alkalis. Moreover, the data from the Durov plot indicates that atmospheric chloride deposition is counterbalanced by increased Na levels resulting from the dissolution of albites and orthoclase. This phenomenon contributes to the prevalence of  $\text{Na}^+ + \text{K}^+$  in groundwater chemistry.

**Figure 7 Durov Diagram Depicting the Dominant Groundwater Types Found in the Study Region**



The Korjinski diagram was employed to ascertain the equilibrium minerals present in the analyzed waters, with assumptions of 25°C temperature and 1 atm pressure, using the DIAGRAMME computer program. As depicted in Figure 8, all samples are situated within the green field, indicative of the kaolinite stability zone. This suggests that kaolinite serves as the predominant secondary phase for the waters within the study region. These results indicate partial weathering of silicate minerals such as biotite and muscovite, suggesting that the groundwater within the aquifer exhibits relatively early to moderately developed flow characteristics and maturity. This inference suggests minimal to no constrained groundwater flow, resulting in insufficient residence time for substantial silica dissolution into the groundwater, as discussed in prior studies (Loh et al., 2016; Obiri-Nyarko et al., 2022).

**Figure 8 The Korjinski Diagram Depicting the Placement of Water Samples Concerning Different Mineral Phases**



### 4.3 Evaluation of the primary factors influencing variations in groundwater chemistry

Table 4 presents the outcomes of Pearson correlation ( $r$ ) analysis. This method offers a concise means to explore relationships between two variables, aiding in drawing meaningful inferences. The Pearson correlation coefficient ( $r$ ) ranges from -1 to 1, representing perfect inverse and direct correlations, respectively (Chegbeleh et al., 2020). Analysis reveals that in the study area, significant contributors to Electrical Conductivity (EC) include Na<sup>+</sup>, Ca<sup>2+</sup>, K<sup>+</sup>, Cl<sup>-</sup>, SO<sub>4</sub><sup>2-</sup> and Mn, as they exhibit correlations exceeding 0.50 with EC. Notably, Sodium and Chloride emerge as primary influencers on EC. Increased mineral dissolution in water leads to heightened availability of electrolytes/ions in groundwater systems, resulting in elevated EC values, potentially influenced by geological factors and/or anthropogenic activities.

Moreover, Na<sup>+</sup> and Cl<sup>-</sup> showed very high correlation ( $r = 0.939$ ). Similarly, SiO<sub>2</sub><sup>-</sup> shows significant negative relation with EC, pH, Na<sup>+</sup>, Cl<sup>-</sup>, SO<sub>4</sub><sup>2-</sup>, and Mn. Among these, SiO<sub>2</sub><sup>-</sup> and EC exhibited the strongest correlation ( $r = -0.875$ ), with EC rising notably as decreasing SiO<sub>2</sub><sup>-</sup>. These show that EC and most parameters do not contribute significantly to SiO<sub>2</sub><sup>-</sup>.

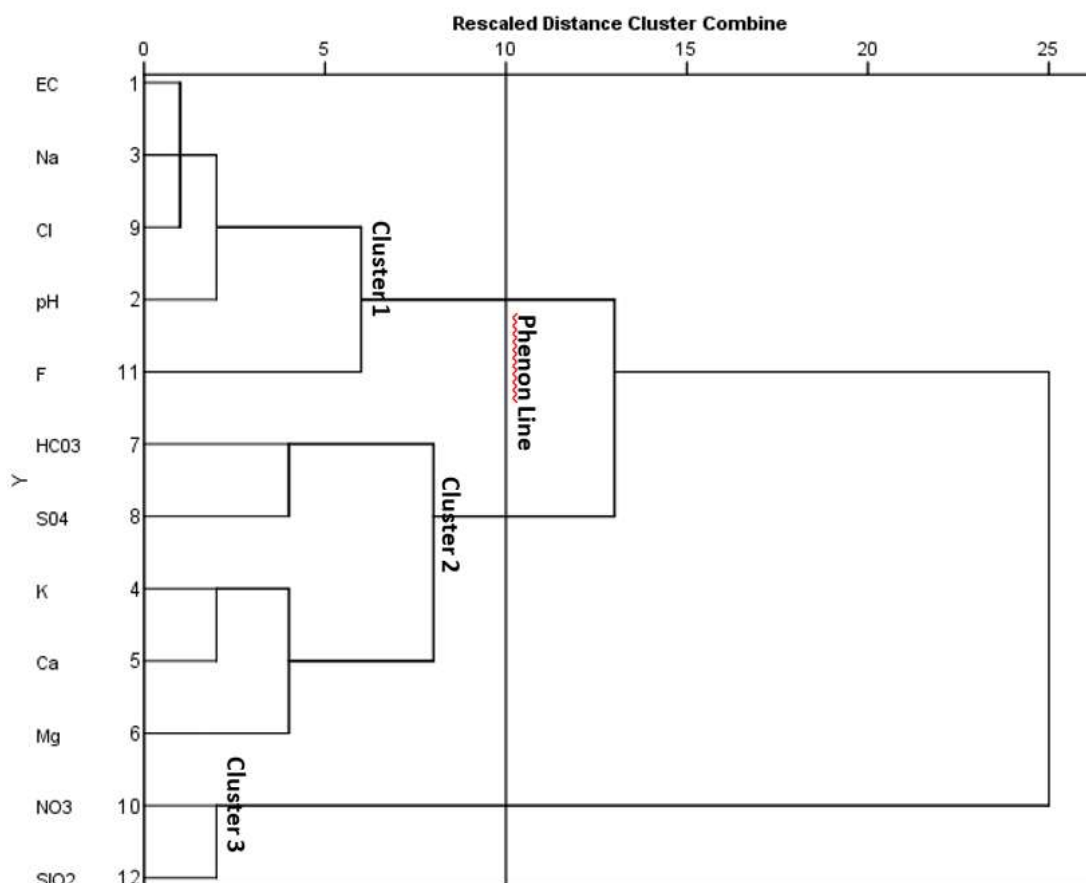
While the connection between F<sup>-</sup> and other parameters remains somewhat unclear, it does exhibit a positive correlation (0.533) with Cl<sup>-</sup>. Additionally, there's a slight positive correlation observed with EC, pH, and sodium. This suggests that F<sup>-</sup> rises as Cl<sup>-</sup> and EC increase within the area.

**Table 4 Pearson Correlation Analysis of Hydrochemical Parameters**

	<b>E</b>	<b>p</b>	<b>Na</b>	<b>K</b>	<b>Ca</b>	<b>M</b>	<b>H</b>	<b>S0</b>	<b>Cl</b>	<b>N</b>	<b>P</b>	<b>F</b>	<b>M</b>	<b>SI</b>	<b>A</b>
	<b>C</b>	<b>H</b>				<b>g</b>	<b>C0</b>	<b>4</b>		<b>O</b>	<b>O</b>		<b>n</b>	<b>O</b>	<b>s</b>
							<b>3</b>			<b>3</b>	<b>4</b>			<b>2</b>	
<b>EC</b>	1														
<b>pH</b>	0.7	1													
	96														
<b>Na</b>	0.9	0.7	1												
	64	81													
<b>K</b>	0.5	0.0	0.4	1											
	25	69	43												
<b>Ca</b>	0.5	0.1	0.4	0.7	1										
	66	81	09	51											
<b>Mg</b>	0.3	0.1	0.2	0.5	0.5	1									
	63	30	48	58	33										
<b>HC</b>	0.1	0.3	0.0	0.1	0.1	0.2	1								
<b>03</b>	76	21	38	15	47	69									
<b>S0</b>	0.6	0.5	0.6	0.3	0.3	0.1	0.4	1							
<b>4</b>	81	84	19	84	58	72	83								
<b>Cl</b>	0.8	0.6	0.9	0.3	0.3	0.2	-	0.4	1						
	85	86	39	85	77	10	0.2	46							
							29								
<b>NO</b>	-	-	-	-	-	-	-	-	-	1					
<b>3</b>	0.7	0.6	0.6	0.4	0.3	0.1	0.1	0.5	0.6						
	03	02	89	11	16	18	79	90	18						
<b>PO</b>	-	-	-	-	-	-	0.0	-	-	0.4	1				
<b>4</b>	0.5	0.4	0.4	0.1	0.2	0.0	11	0.2	0.4	52					
	02	82	26	88	77	42		78	26						
<b>F</b>	0.3	0.3	0.4	-	-	-	-	0.0	0.5	-	-	1			
	30	13	85	0.0	0.2	0.0	0.3	70	33	0.3	0.0				
				17	60	74	71			54	15				
<b>Mn</b>	0.6	0.5	0.7	0.2	0.2	0.1	-	0.1	0.7	-	-	0.4	1		
	68	54	13	36	13	92	0.2	83	65	0.5	0.4	62			
							85			08	50				
<b>SI</b>	-	-	-	-	-	-	-	-	-	0.7	0.4	-	-	1	
<b>O2</b>	0.8	0.8	0.8	0.3	0.3	0.2	0.2	0.6	0.7	20	74	0.4	0.5		
	75	60	51	28	28	36	41	53	77			11	78		
<b>As</b>	0.2	0.4	0.2	-	-	-	-	0.0	0.2	-	-	0.3	0.3	-	1
	32	44	94	0.0	0.2	0.0	0.0	69	51	0.0	0.0	54	82	0.2	
				90	12	87	20			79	92			79	

The application of R-mode Hierarchical Cluster Analysis (HCA) and factor analysis has unveiled broad field associations shedding light on the variations in groundwater chemical composition within the research region. The R-mode cluster analysis procedure mirrored that of Q-mode cluster analysis. Figure 9 displays the dendrogram derived from the R-mode HCA, with the phenon line delineated at a linkage distance of 10, yielding three distinct clusters representing predominant groundwater relationships and mechanisms influencing groundwater characteristics. Cluster 1 comprising EC,  $\text{Na}^+$ ,  $\text{Cl}^-$ ,  $\text{F}^-$  and pH suggests a correlation among these parameters. Elevated levels of EC,  $\text{Na}^+$  and  $\text{Cl}^-$ , potentially signify accessory mineral dissolution in both saturated and unsaturated zones. Fluoride concentration in groundwater can be influenced by geochemical phenomena such as mineral dissolution, precipitation, adsorption-desorption reactions, and ion exchange, with pH playing a pivotal role in these processes by impacting fluoride ion solubility and mobility. Cluster 2 encompasses  $\text{HCO}_3^{2-}$ ,  $\text{SO}_4^{2-}$ ,  $\text{Ca}^{2+}$ ,  $\text{K}^+$ , and  $\text{Mg}^{2+}$ , indicative of diverse geochemical processes including carbonate mineral weathering, gypsum dissolution, and cation exchange reactions. This cluster likely represents natural groundwater chemistry influenced by interactions between rocks and water, as well as mineral dissolution. Cluster 3, associating  $\text{NO}_3^-$  and  $\text{SiO}_2$ , displays closer linkage distances compared to other clusters, suggesting greater similarity among its constituents. This indicates similarities in concentration or sources within the groundwater system. Nitrate contamination, often stemming from agricultural practices like fertilizer use or livestock operations, and silica concentrations reflecting silicate mineral weathering in the aquifer, provide valuable insights into subsurface hydrogeochemical processes.

**Figure 9 Dendrogram For R-Mode Cluster Analysis**





In alignment with the outcomes of R-mode Hierarchical Cluster Analysis (HCA), the R-mode factor analysis yielded 3 factors within the final model, collectively explaining approximately 82% of the overall variability in groundwater chemistry (refer to Table 5). Corresponding loadings for each parameter are presented in Table 6. The validity of the factor model is contingent upon high communalities among parameters. To ensure robustness, a stringent minimum threshold of 0.5 was established within the scope of this research, necessitating the exclusion of variables with communalities below this threshold. Consequently, exclusively those variables exerting meaningful influences on the alignment with independent factors were retained in the final model. Mn, Fe,  $\text{PO}_4^-$  and As (Table 7) were excluded from multivariate analyses due to their concentrations being largely below detectable levels across most locations. Notably, in Table 6  $\text{F}^-$  was omitted from the final factor model as it displayed high loadings across multiple components.

The first component, explaining over 46% of the overall variability in the chemical composition of groundwater within the investigated region, exhibits notably positive loadings for EC, pH,  $\text{Na}^+$ ,  $\text{SO}_4^{2-}$ , and  $\text{Cl}^-$ , alongside negative loadings for  $\text{NO}_3^-$  and  $\text{SiO}_2^-$ . This component, derived through correlation analysis, HCA, and PCA, reflects the breakdown of secondary minerals in both saturated and unsaturated zones. The considerable positive loadings of  $\text{Na}^+$  and  $\text{Cl}^-$  suggest their significant contribution to salinity levels (EC) in the study area. Furthermore, the presence of  $\text{Cl}^-$  and  $\text{SO}_4^{2-}$  ions in Factor 1 implies the potential influence of anthropogenic activities stemming from industrial and agricultural waste components. An examination through a Sodium-Chloride plot (Fig. 10) indicates that while halite breakdown contributes to dissolved  $\text{Na}^+$  levels within the aquifer system, it doesn't solely account for all  $\text{Na}^+$  enrichment. Instead, ion exchange reactions and additional mineral weathering mechanisms rich in Na are implicated in aquifer  $\text{Na}^+$  enrichment, with halite dissolution confined to specific geological regions. Besides halite dissolution, atmospheric aerosol dissolution in precipitation stands as the sole source of  $\text{Cl}^-$  in aquifers (Yidana et al., 2012). Figure 11 unveils another facet: the relationship between  $\text{Ca}^{2+}$  concentration and  $\text{HCO}_3^-$ , suggesting a potential involvement of cation exchange in shaping hydrochemistry. The negative loading of  $\text{SiO}_2^-$  with component 1 indicates that silica in groundwater minimally contributes to electrical conductivity, consistent with correlation analysis outcomes. Component 2, representing approximately 22% of total variation, demonstrates high loadings with  $\text{Ca}^{2+}$ ,  $\text{K}^+$ , and  $\text{Mg}^{2+}$  indicating their presence due to dolomite dissolution and cation exchange processes. The third factor, accounting for about 14% of variability, exhibits significant positive loadings for  $\text{HCO}_3^{2-}$ , signifying the prevalence of carbonate minerals within the groundwater system.

**Table 5 Pearson's Correlation Matrix Between Water Quality Parameters  
Total Variance Explained**

Initial Eigenvalues				Extraction Sums of Squared Loadings				Rotation Sums of Squared Loadings			
				Total							
				1							
Component	Total	% of Variance	Cumulative %	Component	Total	% of Variance	Cumulative %	Component	Total	% of Variance	Cumulative %
t	l	e	e %	e	e %	e	e %	l	e	e	e %

1	6.16 9	51.410	51.410	6.16 9	51.410	51.410	5.50 8	45.902	45.902
2	2.16 0	18.002	69.412	2.16 0	18.002	69.412	2.59 2	21.597	67.499
3	1.47 5	12.291	81.703	1.47 5	12.291	81.703	1.70 5	14.204	81.703
4	.680	5.663	87.366						
5	.570	4.749	92.115						
6	.345	2.874	94.989						
7	.211	1.760	96.750						
8	.157	1.305	98.054						
9	.128	1.063	99.117						
10	.075	.629	99.746						
11	.022	.182	99.928						
12	.009	.072	100.000						

**Table 6 Final Factor Loadings for the Water Quality Parameters  
Rotated Component Matrix<sup>a</sup>**

	Component		
	1	2	3
EC	.889	.413	-.015
pH	.902	-.060	.186
Na	.915	.281	-.173
K	.224	.877	-.024
Ca	.202	.882	.106
Mg	.085	.744	.131
HC03	.186	.070	.924
S04	.701	.203	.444
Cl	.832	.272	-.408
NO3	-.778	-.180	-.034
SIO2	-.930	-.149	-.063

**Table 7 Communalities of Parameters on Factor Model  
Communalities**

	Initial	Extraction
EC	1.000	.962
pH	1.000	.851
Na	1.000	.947

K	1.000	.820
Ca	1.000	.831
Mg	1.000	.578
HC03	1.000	.893
S04	1.000	.730
Cl	1.000	.934
NO3	1.000	.639
SIO2	1.000	.892

Extraction Method: Principal Component Analysis.

**Figure 10 Graph of Na<sup>+</sup> Against Cl<sup>-</sup> Illustrating Silicate Mineral Dissolution and Reverse Cation Exchange Processes**

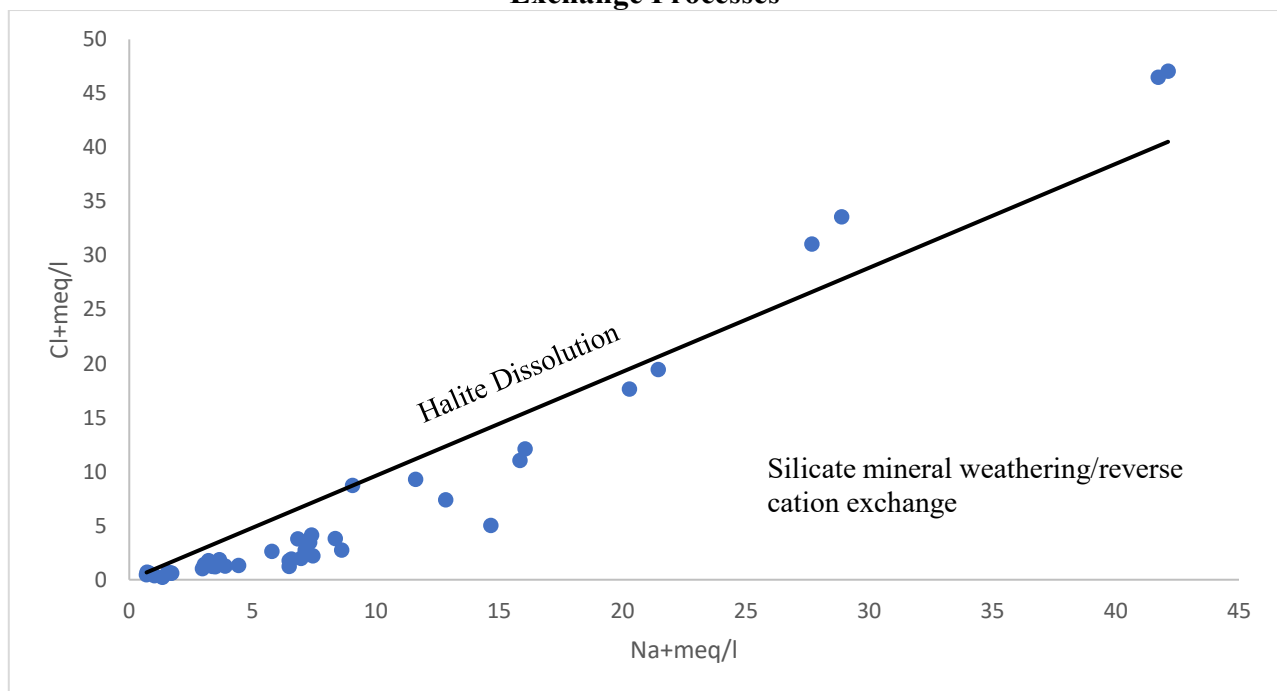
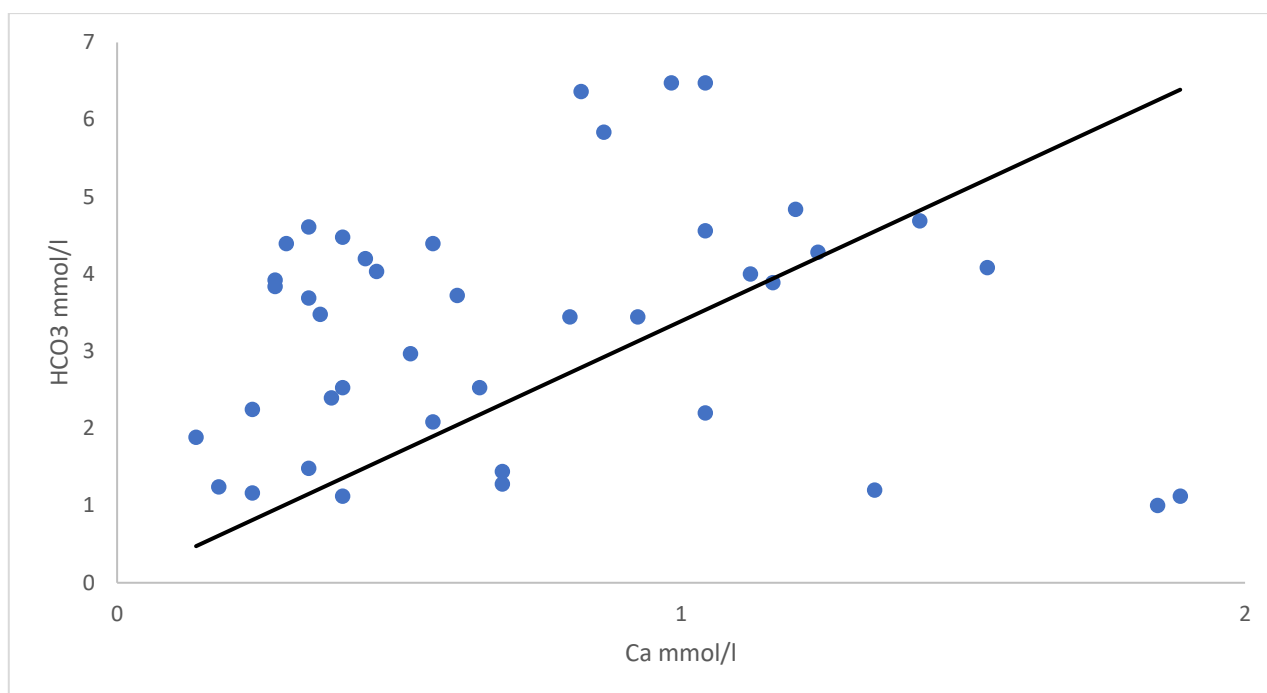


**Figure 11 Scatterplot of Ca Against HCO<sub>3</sub> Highlighting the Extent of Cation Exchange Influencing the Hydrochemical Composition**



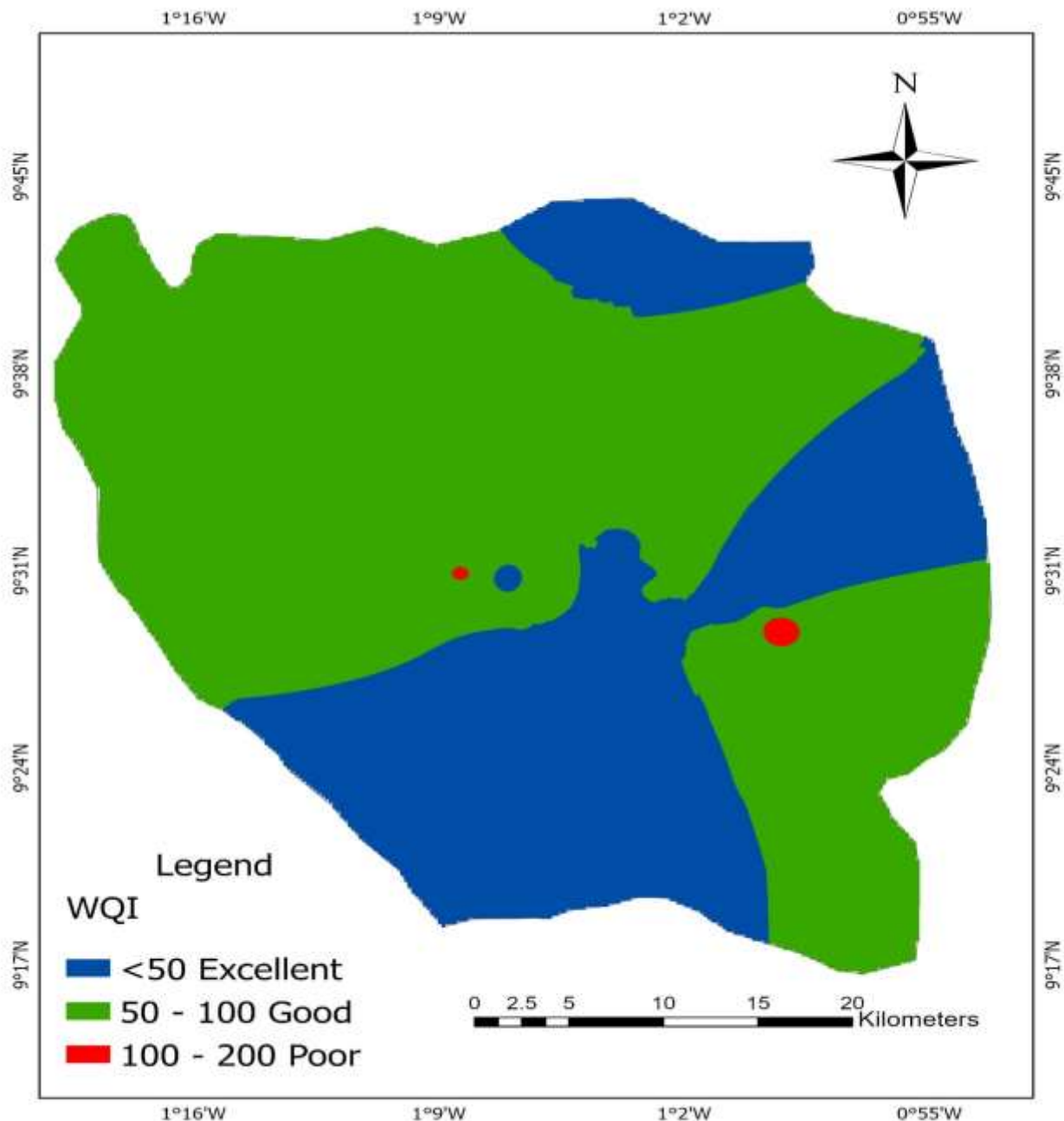
#### 4.4 Evaluation of Groundwater Chemical Quality for Potable Use

The availability of clean water is not only a fundamental human right but also a crucial catalyst for socioeconomic progress in many nations. By mitigating adverse health effects and reducing healthcare expenses, reliable access to quality water significantly contributes to overall development. Given that groundwater functions as the primary supply for drinking and household needs in the district, a thorough examination of certain chemical parameters with significant health implications is imperative to ascertain its suitability for such essential uses.

To facilitate this assessment, Water Quality Indices were calculated and spatially interpolated using an inverse distance weighting procedure. This interpolation method was chosen based on its superior performance, evidenced by the smallest root mean square error, as highlighted in previous studies (Loh et al., 2020).

Based on the spatial prediction map (Figure 12), it is evident that the chemical quality of groundwater in the district generally meets the standards for domestic use. Particularly, groundwater in the southwestern and northeastern areas stands out for its excellent quality. The estimated Water Quality Indices (WQIs) range from 22.40 to 145.85, with approximately 68% of the water falling into the "excellent" category for drinking purposes, while 22% and 10% are classified as "good" and "poor" quality, respectively (Figure 12). The areas of poor water quality, identified in Wantugu, Tanshegu, and Voggu, are characterized by elevated levels of  $F^-$ , As, and chloride. The analyzed water samples exhibit elevated Total Dissolved Solids, Electrical Conductivity, and pH values, suggesting localized release of these ions into the groundwater, serving as a possible source of contamination.

**Figure 12 Spatial Distribution of Water Quality Indices**



#### 4.5 An assessment of the suitability of groundwater for irrigation

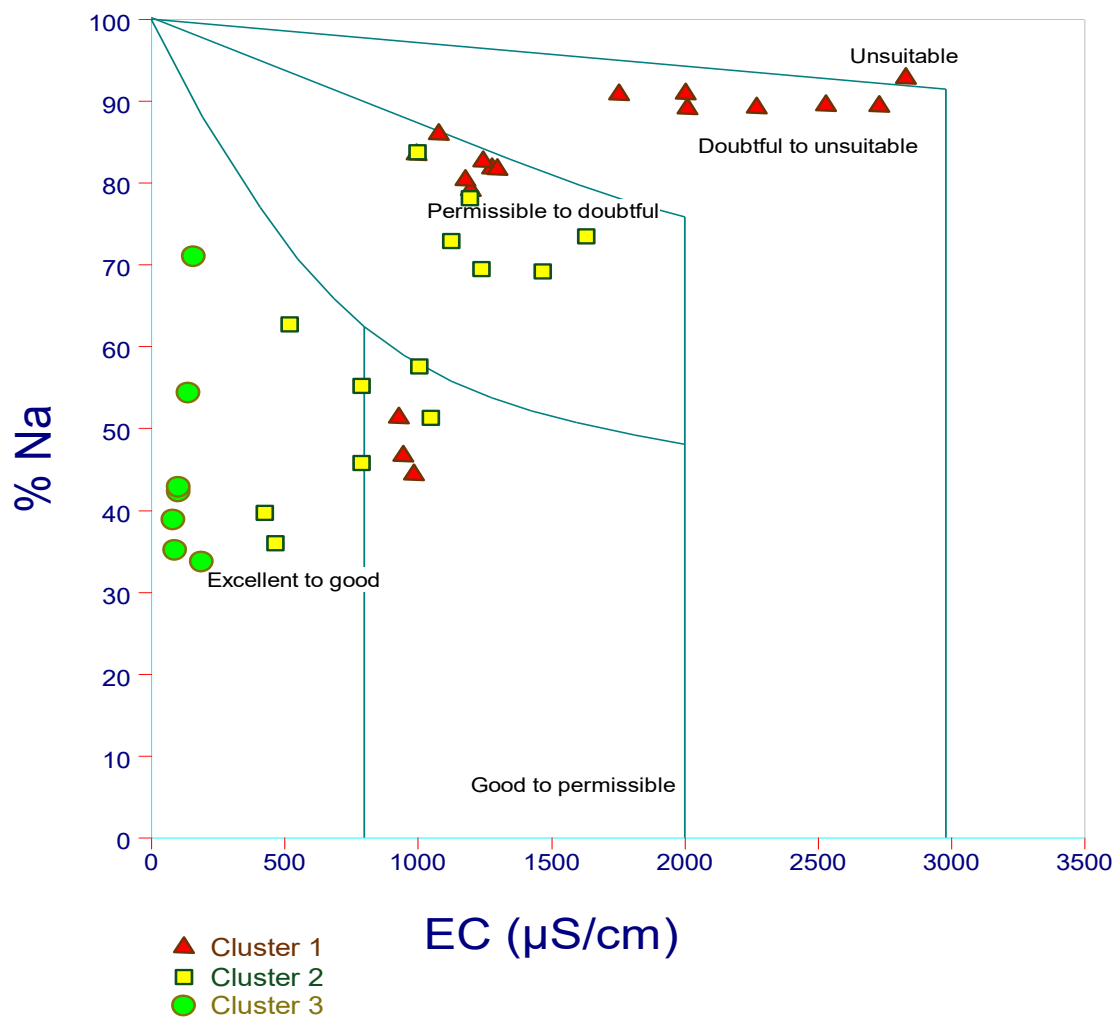
The quality of water utilized for irrigation plays a pivotal role in crop yield, soil productivity, and environmental preservation. Hence, evaluating the appropriateness of water for irrigation should focus on indicators that forecast potential soil conditions harmful to plant development or harmful to humans and animals consuming these crops. Water with high salinity and  $\text{Na}^+$  levels is unsuitable for irrigation as excessive salinity diminishes plant osmotic activity, hampering water and nutrient absorption from the soil. Elevated sodium levels, particularly in irrigation water, can harm certain soil types. This diminishes soil permeability and disrupts soil structure, impeding water infiltration into the soil and potentially compromising plant growth and productivity, as highlighted by Kumar et al. (2006). However, in



appropriate proportions, calcium and magnesium can counteract the detrimental effects of sodium on soil, serving as a buffer.

The Wilcox (1955) diagram serves as a tool for classifying irrigation water quality based on sodium content. According to the diagram (Figure 13), approximately 29% of groundwater samples, primarily composed of Clusters 1 and 2, fall within the 'Excellent to good' irrigation water category. Additionally, five samples are categorized as 'good to permissible' irrigation water, indicating groundwater suitability for irrigation purposes. Roughly 32% of samples fall within the 'permissible to doubtful' category, suggesting potential suitability for irrigation. However, samples from Cluster 3 are situated within the 'doubtful to unsuitable' category, implying that prolonged use of lake water for irrigation may lead to sodium accumulation on soil particles, resulting in soil clay swelling/dispersion, surface crusting, and pore clogging over time, as noted by Bauder et al. (2011). Consequently, Cluster 3 samples are unsuitable for irrigation or should be limited to salt-tolerant crops and soil types with high permeability and minimal susceptibility to sodicity-related issues.

**Figure 13 Groundwater Quality Assessment for the Study Area Based on Wilcox (1955) Diagram.**



## 5 Conclusion

The findings of this study shed light on the primary influences the chemical composition of groundwater within the Tolon-Kumbungu District and its appropriateness for different uses. Through a combination of multivariate statistical techniques and traditional graphical approaches used on groundwater samples, it was observed that the dissolution of silicate minerals, along with the impact of industrial waste and agricultural waste, represent the primary influences shaping the composition of groundwater in the region. Q-mode Hierarchical Cluster Analysis (HCA) identified three distinct groundwater flow regimes: recharge zones (cluster 1) situated in high-altitude regions, characterized by minimal Total Dissolved Solids and predominantly composed of Na-Mg-  $\text{HCO}_3$  water type; transition zones (cluster 2) dominated by Na- $\text{HCO}_3$  water type; and Na-Cl water type (cluster 3) in discharge regions. Evaluation of Water Quality Indices (WQIs) suggests that the groundwater in the area is mostly appropriate for domestic use, with 90% of samples classified as good to excellent in quality, and only 10% falling within the poor category. For irrigation purposes, groundwater from Cluster 1, which typically exhibits low salinity, is identified as the most favorable.

## References

1. Abagale F. K., Osei R.A., Antwi P. K., “Water Quality Variation of Selected Open Wells and Boreholes in Tolon District of Northern Ghana”, *International Journal of Current Research*, 2020, 12 (05), 11748-11754.
2. Abagale F. K., Yusif H., Abagale S.A., “Nutrient Concentration in Surface Water from Crop Lands in the Tolon District, Ghana”, *Asian Journal of Science and Technology*, 2020, 11, (06), 10985-10991.
3. Abanyie S.K., Apea O. B., Abagale S. A., Amuah E. E. Y., Sunkari E. D., “Sources and factors influencing groundwater quality and associated health implications: A review”, *Emerging Contaminants*, 2023, 9(2), 100207. <https://doi.org/10.1016/j.emcon.2023.100207>
4. Abdul-Ganiyu S., Hirohiko I., Adongo T. A., Kranjac-Berisavljevic G., “Evaluating Borehole Performance in Tolon and Wa West Districts of Northern Ghana”, *African Journal of Applied Research*, 2017, 3(2), 73-84.
5. Agodzo S. K., Bessah E., Nyatuame M., “A review of the water resources of Ghana in a changing climate and anthropogenic stresses, *Frontiers in Water*”, 2023, 4, 973825.
6. Akhtar N., Syakir Ishak M. I., Bhawani S. A., Umar, K., “Various Natural and Anthropogenic Factors Responsible for Water Quality Degradation: A Review” *Water*, 2021, 13(19), 2660.
7. Aljumily R., “Agglomerative hierarchical clustering: an introduction to essentials. (1) proximity coefficients and creation of a vector-distance matrix and (2) construction of the hierarchical tree and a selection of methods,” *Global Journal of Human-Social Science*, 2021, 16 (3) 22–50.
8. Amuah E. E. Y., Boadu J. A., Nandomah, S., *Emerging issues and approaches to protecting and sustaining surface and groundwater resources: emphasis on Ghana. Groundwater for Sustainable Development*, 2022, 16, 100705.
9. Aragaw T. T., Gnanachandrasamy G., “Evaluation of groundwater quality for drinking and irrigation purposes using GIS-based water quality index in urban area of Abaya-Chemo sub-basin of Great Rift Valley, Ethiopia,” *Applied Water Science*, 2021, 11(9), 148.
10. Asare-Donkor N. K., Adimado, A. A., “Groundwater quality assessment in the Northern and Upper East Regions of Ghana”, *Environmental Earth Sciences*, 2020, 79(10), 205.

11. Banoeng-Yakubo B., Yidana S.M., Nti E., “An evaluation of the genesis and suitability of groundwater for irrigation in the Volta Region”. *Environmental Geology*, 2009, 57 (5), 1005–1010. <https://doi.org/10.1007/s00254-008-1185-y>
12. Bauder T. A., Waskom R.M., Sutherland P.L., Davis J. G., “Irrigation water quality criteria”, Colorado State University Extension, 2011.
13. Brown R.M., McClelland N.J., Deiniger R.A., O’Connor M.F.A., “Water quality index – crossing the physical barrier”, In: Jenkins, S.H. (Ed.), *Proceedings in International Conference on Water Pollution Research Jerusalem*, 1972, 6, 787–797.
14. Çadraku, H. S., “Groundwater quality assessment for irrigation: case study in the Blinaja river basin, Kosovo”, *Civil Engineering Journal*, 2021, 7(9), 1515-1528.
15. Chaudhuri R., Sahoo S., Debsarkar A., Hazra S., “Fluoride Contamination in Groundwater—A Review”, *Geospatial Practices in Natural Resources Management*, 2024, 331-354.
16. Chegbele L. P., Aklika D. K., Akurugu B. A., “Hydrochemical characterization and suitability assessment of groundwater quality in the Saboba and Chereponi Districts”, *Ghana. Hydrology*, 2020, 7(3), 53.
17. Chegbele L. P., Akurugu B. A., Yidana S. M., “Assessment of groundwater quality in the Talensi District, Northern Ghana”, *The scientific world Journal*, 2020, 24, <https://doi.org/10.1155/2020/8450860>
18. Cobbina S.J. Armah F.A., Obiri S., *Multivariate Statistical and Spatial Assessment of Groundwater Quality in the Tolon-Kumbungu District, Ghana*, *Research Journal of Environmental and Earth Sciences*, 2012, 4(1), 88-98.
19. CWSA Tamale, *Water quality, pollution & the impact of polluted water in rural areas*, In S. E. (author) (Ed.) 2023.
20. Dhaouadi L., Besser H., Wassar F., Kharbout N., Brahim N. B., Wahba M. A., Kang Y. K., “Agriculture sustainability in arid lands of southern Tunisia: Ecological impacts of irrigation water quality and human practices”, *Irrigation and Drainage*, 2020, 69(5), 974-996.
21. Dorleku M. K., Nukpezah D., Carboo D., “Effects of small-scale gold mining on heavy metal levels in groundwater in the Lower Pra Basin of Ghana”. *Applied Water Science*, 2018, 8, 126. <https://doi.org/10.1007/s13201-018-0773-z>
22. Erga, S., “Affordable water treatment solutions for domestic use: a community dugout in the Tolon district, Ghana”, (Master's thesis, Norwegian University of Life Sciences), 2023.
23. Ferrer N., Folch A., Masó, G., Sanchez S., Sanchez-Vila X., “What are the main factors influencing the presence of faecal bacteria pollution in groundwater systems in developing countries?”, *Journal of Contaminant Hydrology*, 2020, 228, 103556. <https://doi.org/10.1016/j.jconhyd.2019.103556>
24. Gao Z., Han C., Xu Y., Zhao Z., Luo Z., Liu, J., “Assessment of the water quality of groundwater in Bohai Rim and the controlling factors—A case study of northern Shandong Peninsula, north China,” *Environmental Pollution*, 2021, 285, 117482. <https://doi.org/10.1016/j.envpol.2021.117482>
25. Ghana Statistical Service GSS., “Water and Sanitation”, 2022, [https://statsghana.gov.gh/gssmain/fileUpload/pressrelease/Volume%203M\\_Water%20and%20Sanitation\\_240222a.pdf](https://statsghana.gov.gh/gssmain/fileUpload/pressrelease/Volume%203M_Water%20and%20Sanitation_240222a.pdf)

26. Hagan G. B., Minkah R., Yiran G. A., Dankyi E., “Assessing groundwater quality in peri-urban Accra, Ghana: Implications for drinking and irrigation purposes”, *Groundwater for Sustainable Development*, 2022, 17, 100761. <https://doi.org/10.1016/j.gsd.2022.100761>
27. Hossain M., Patra P. K., “Hydrogeochemical characterisation and health hazards of fluoride enriched groundwater in diverse aquifer types”, *Environmental Pollution*, 2020, 258, 113646. <https://doi.org/10.1016/j.envpol.2019.113646>
28. Jeil E. B., Abass K., Ganle, J. K., ““We are free when water is available”: gendered livelihood implications of sporadic water supply in Northern Ghana”, *Local Environment*, 2020, 25(4), 320-335.
29. Kokkat A., Palanichamy J., Joseph J.E., “Spatial and Temporal Variation in Groundwater Quality and Impact of Sea Water in the Cauvery Delta, South India”, *International Journal of Earth Sciences and Engineering*, 2016, 9, 383–392.
30. Krishna B., Achari V. S., “Groundwater for Drinking and Industrial Purposes: A Study of Water Stability and Human Health Risk Assessment from Black Sand Mineral Rich Coastal Region of Kerala, India”, *Journal of Environmental Management*, 2024, 351, 119783. <https://doi.org/10.1016/j.jenvman.2023.119783>
31. Kumar M., Ramanathan A.L., Rao S., Kumar B., “Identification and Evaluation of Hydrogeochemical Processes in the Groundwater Environment of Delhi, India”, *Environmental Geology*, 2006, 50 (7), 1025–1039.
32. Lee J. M., Koh D. C., Chae G. T., Kee W. S., Ko K. S., “Integrated Assessment of Major Element Geochemistry and Geological Setting of Traditional Natural Mineral Water Sources in South Korea at the National Scale”, *Journal of Hydrology*, 2021, 598, 126249.
33. Loh Y. S. A., Akurugu B. A., Manu E., Aliou A., “Assessment of Groundwater Quality and the Main Controls on Its Hydrochemistry in Some Voltaian and Basement Aquifers, Northern Ghana”, *Groundwater for Sustainable Development*, 2020, 10, 100296. <https://doi.org/10.1016/j.gsd.2019.100296>
34. Loh Y.S.A., Yidana S.M., Banoeng-Yakubo B., Sakyi P.A., Addai M.O., Asiedu D.K., “Determination of the Mineral Stability Field of Evolving Groundwater in the Lake Bosomtwi Impact Crater and Surrounding Areas”, *Journal of African Earth Sciences*, 2016, 121, 286–300.
35. Luvhimbi N., Tshitangano T. G., Mabunda J. T., Olaniyi F. C., Edokpayi J. N., “Water Quality Assessment and Evaluation of Human Health Risk of Drinking Water from Source to Point of Use at Thulamela Municipality, Limpopo Province”, *Scientific Reports*, 2022, 12 (1), 6059.
36. Mahjoub O., Mauffret A., Michel C., Chmingui W., “Use of Groundwater and Reclaimed Water for Agricultural Irrigation: Farmers’ Practices and Attitudes and Related Environmental and Health Risks”, *Chemosphere*, 2022, 295, 133945. <https://doi.org/10.1016/j.chemosphere.2022.133945>
37. Masindi V., Foteinis S., “Groundwater Contamination in Sub-Saharan Africa: Implications for Groundwater Protection in Developing Countries”, *Cleaner Engineering and Technology*, 2021, 2, 100038. <https://doi.org/10.1016/j.clet.2020.100038>
38. Massally R-E.M., Sheriff A.B., Kaitibi D., Abu A., Barrie M., Taylor E.T., “Comprehensive Assessment of Groundwater Quality Around a Major Mining Company in Southern Sierra Leone”, *Journal of Water Resource and Protection*, 2017, 9, 601–613.
39. Mather J., “Relationship Between Rock, Soil, and Groundwater Compositions”, in *Geochemical Processes, Weathering and Groundwater Recharge in Catchments*, CRC Press, 2020, pp. 305–328.

40. Mukherjee I., Singh U.K., “Fluoride Abundance and Their Release Mechanisms in Groundwater Along with Associated Human Health Risks in a Geologically Heterogeneous Semi-Arid Region of East India”, *Microchemical Journal*, 2020, 152, 104304.
41. Mummuni A.N., Bayor J.S., “Groundwater Prospecting Using the Dipole-Dipole Configuration for Vertical Electrical Sounding: Prediction of Major Aquifer Depth in the Tolon-Kumbungu District of Northern Ghana”, *Journal of Science and Technology*, 2017, 37 (2), 43–58.
42. Nigam N., Kumar S., “Contamination of Water Resources: With Special Reference to Groundwater Pollution”, *Current Directions in Water Scarcity Research*, 2022, 5, 169–186. <https://doi.org/10.1016/B978-0-323-85378-1.00010-6>
43. Obiri-Nyarko F., Asugre S.J., Asare S.V., Duah A.A., Karikari A.Y., Kwiatkowska-Malina J., Malina G., “Hydrogeochemical Studies to Assess the Suitability of Groundwater for Drinking and Irrigation Purposes: The Upper East Region of Ghana Case Study”, *Agriculture*, 2022, 12, 1973.
44. Piper A.M., “A Graphic Procedure in Geochemical Interpretation of Water Analysis”, *Transactions of the American Geophysical Union*, 1944, 25 (6), 914–928.
45. Qureshi S.S., Channa A., Memon S.A., Khan Q., Jamali G.A., Panhwar A., Saleh T.A., “Assessment of Physicochemical Characteristics in Groundwater Quality Parameters”, *Environmental Technology & Innovation*, 2021, 24, 101877. <https://doi.org/10.1016/j.eti.2021.101877>
46. Ram A., Tiwari S.K., Pandey H.K., Chaurasia A.K., Singh S., Singh Y.V., “Groundwater Quality Assessment Using Water Quality Index (WQI) Under GIS Framework”, *Applied Water Science*, 2021, 11, 1–20.
47. Ren C., Zhang Q., “Groundwater Chemical Characteristics and Controlling Factors in a Region of Northern China with Intensive Human Activity”, *International Journal of Environmental Research and Public Health*, 2020, 17 (23), 9126.
48. Sahu P., Sikdar P.K., “Hydrochemical Framework of the Aquifer in and Around East Kolkata Wetlands, West Bengal, India”, *Environmental Geology*, 2008, 55, 823–835.
49. Samaei F., Emami H., Lakzian A., “Assessing Soil Quality of Pasture and Agriculture Land Uses in Shandiz County, Northwestern Iran”, *Ecological Indicators*, 2022, 139, 108974.
50. Sangwan P., Rishi M.S., Singh G., “Assessment of Drinking Water Quality and Non-Carcinogenic Health Risk Associated with the Feed and Treated Water of Water Treatment Devices (WTDs) in Southwest Punjab, India”, *Toxin Reviews*, 2022, 41 (2), 536–550.
51. Sankoh A.A., Komba T., Laar C., Derkyi N.S.A., Frazer-Williams R., “Application of Multivariate and Geospatial Techniques to Assess Groundwater Quality of Two Major Dumpsites in Sierra Leone”, *Environmental Nanotechnology, Monitoring & Management*, 2022, 18, 100753.
52. Sasakova N., Gregova G., Takacova D., Mojziso J., Papajova I., Venglovsky J., Szaboova T., Kovacova S., “Pollution of Surface and Ground Water by Sources Related to Agricultural Activities”, *Frontiers in Sustainable Food Systems*, 2018, 2, 370488. <https://doi.org/10.3389/fsufs.2018.00042>
53. Seidu J., Ewusi A., “Assessment of Groundwater Quality Using Hydrogeochemical Indices and Statistical Analysis in the Tarkwa Mining Area of Ghana”, *Journal of Environmental Hydrology*, 2018, 26 (1), 1–10.
54. Snousy M.G., Wu J., Su F., Abdelhalim A., Ismail E., “Groundwater Quality and Its Regulating Geochemical Processes in Assiut Province, Egypt”, *Exposure and Health*, 2022, 14 (2), 305–323.



55. Sunkari E.D., Seidu J., Ewusi A., “Hydrogeochemical Evolution and Assessment of Groundwater Quality in the Togo and Dahomeyan Aquifers, Greater Accra Region, Ghana”, *Environmental Research*, 2022, 208, 112679. <https://doi.org/10.1016/j.envres.2022.112679>
56. USGS, “National Field Manual for the Collection of Water-Quality Data: U.S. Geological Survey Techniques of Water-Resources Investigations Book 9, Chaps. A1–A10”, United States Geological Survey, 2006. A1-A10. <http://pubs.water.usgs.gov/twri9A>
57. Viero A.P., Roisenberg C., Roisenberg A., Vigo A., “The Origin of Fluoride in the Granitic Aquifer of Porto Alegre, Southern Brazil”, *Environmental Geology*, 2009, 56 (9), 1707–1719.
58. Wali S.U., Gada M.A., Hamisu I., Umar K.J., Abor I.G., “Evaluation of Shallow Groundwater in Rural Kebbi State, NW Nigeria, Using Multivariate Analysis: Implication for Groundwater Quality Management”, *MOJ Ecology and Environmental Sciences*, 2022, 7 (3), 65–75.
59. Walker J.S., “Sustainable Safe Water and Sanitation Interventions in Remote Parts of Ghana”, In: Rajapakse J. (ed.) *Safe Water and Sanitation for a Healthier World, Sustainable Development Goals Series*, Springer, Cham, 2022, 93–116. [https://doi.org/10.1007/978-3-030-94020-1\\_5](https://doi.org/10.1007/978-3-030-94020-1_5)
60. Wang B.B., “Research on Drinking Water Purification Technologies for Household Use by Reducing Total Dissolved Solids (TDS)”, *PLOS ONE*, 2021, 16 (9), e0257865.
61. WHO, “Guidelines for Drinking-Water Quality: Fourth Edition Incorporating the First Addendum”, World Health Organization, 2017.
62. Wilcox L.V., “Classification and Use of Irrigation Waters”, USDA Circular No. 969, 1955, 1–19.
63. Yadav M., Singh G., Jadeja R.N., “Fluoride Contamination in Groundwater, Impacts, and Their Potential Remediation Techniques”, *Groundwater Geochemistry: Pollution and Remediation Methods*, 2021, 22–41.
64. Yeleliere E., Cobbina S.J., Duwiejuah A.B., “Review of Ghana’s Water Resources: The Quality and Management with Particular Focus on Freshwater Resources”, *Applied Water Science*, 2018, 8 (1), 1–12.
65. Yidana S.M., Dzikunoo E.A., Aliou A., Adams R.M., Chagbeleh L.P., Anani C., “The Geological and Hydrogeological Framework of the Panabako, Kodjari, and Bimbilla Formations of the Voltaian Supergroup – Revelations from Groundwater Hydrochemical Data”, *Applied Geochemistry*, 2020, 115, 104533. <https://doi.org/10.1016/j.apgeochem.2020.104533>
66. Yidana S.M., Banoeng-Yakubo B., Akabzaa T.M., “Analysis of Groundwater Quality Using Multivariate and Spatial Analysis in the Keta Basin, Ghana”, *Journal of African Earth Sciences*, 2010, 58 (2), 220–234.
67. Yidana S.M., Banoeng-Yakubo B., Aliou A.S., Akabzaa T., “Groundwater Quality in Some Voltaian and Birimian Aquifers in Northern Ghana—Application of Multivariate Statistical Methods and Geographic Information Systems”, *Hydrological Sciences Journal*, 2012, 57 (6), 1168–1183.
68. Yidana S.M., Banoeng-Yakubo B., Akabzaa T., Asiedu D., “Characterisation of the Groundwater Flow Regime and Hydrochemistry of Groundwater from the Buem Formation, Eastern Ghana”, *Hydrological Processes*, 2011, 25 (14), 2288–2301.